Available online at www.sciencedirect.com
ScienceDirect
Coordination Chemistry Reviews 251 (2007) 1128–1157
COORDINATION CHEMISTRY REVIEWS
www.elsevier.com/locate/ccr

Review

Ruthenium phthalocyanine and naphthalocyanine complexes: Synthesis, properties and applications

Tristan Rawling, Andrew McDonagh *

Institute of Nanoscale Technology, University of Technology Sydney, Sydney 2007, Australia

Received 30 June 2006; accepted 29 September 2006
Available online 5 October 2006

Contents

1. Introduction 1129
2. Synthesis 1129
   2.1. Synthesis of complexes with unsubstituted phthalocyanine macrocycles 1129
      2.1.1. Ring-forming syntheses 1129
      2.1.2. Synthesis by incorporation of Ru into the phthalocyanine macrocycle 1132
      2.1.3. Synthesis involving axial ligand substitution 1132
      2.1.4. Dimeric and polymeric complexes 1133
   2.2. Synthesis of complexes with substituted phthalocyanine macrocycles 1134
      2.2.1. Substituted ring-forming syntheses 1134
      2.2.2. Synthesis involving zeolites and molecular sieves 1135
      2.2.3. Synthesis by incorporation of Ru into a substituted macrocycle 1135
      2.2.4. Synthesis involving axial ligand substitution 1136
      2.2.5. Substituted dimeric and polymeric complexes 1138
   2.3. Synthesis of naphthalocyanine complexes 1139
3. Properties of ruthenium phthalocyanine and naphthalocyanine complexes 1140
   3.1. Spectroscopic properties 1140
      3.1.1. UV–vis absorption spectra 1140
      3.1.2. Infra-red spectra 1141
      3.1.3. NMR spectra 1142
   3.2. Redox chemistry 1143
      3.2.1. Formal oxidation states of Ru in phthalocyanine complexes 1143
      3.2.2. Electrochemistry 1143
      3.2.3. Chemical redox properties 1145
      3.2.4. Photo-redox properties 1146
   3.3. Structural properties 1146
      3.3.1. Single-crystal X-ray diffraction studies 1146
      3.3.2. Structural properties of powders and films 1147

Abbreviations: 3-atri, 3-amino-1,2,4-triazine; 5-atri, 5-amino-1,2,4-triazine; 3-Clpy, 3-chloropyridine; 3-Fpy, 3-fluoropyridine; apy, 4-aminopyridine; bpy, 4,4′-bipyridine; bpyac, 4,4′-bipyridylacetylene; Bupy, butylpyridine; tBu$_2$dib, 2,5-di-t-butyl-1,4-diisocyanobenzene; tBupyz, 2-t-butylpyrazine; $(C_8H_{17})_2$dib, 2,5-dioctyl-1,4-diisocyanobenzene; $(C_{10}H_{21})_2$dib, 2,5-didecyl-1,4-diisocyanobenzene; $(CN)_2C_6F_4$, 2,3,5,6-tetrafluoro-1,4-dicyanobenzene; Cl$_2$tz, 3,6-dichloro-s-tetrazine; Cl$_4$dib, 2,3,5,6-tetrachloro-1,4-diisocyanobenzene; Clpyz, 2-chloropyrazine; dabco, 1,4-diazabicyclo[2.2.2]octane; daf, 2,7-diaminofluorene; datz, diamin-s-otetrazine; DBU, 1,8-diazabicyclo[5,4,0]unde-7-cene; dia, 9,10-diisocyanoanthracene; dib, 1,4-diisocyanobenzene; dmf, dimethylformamide; dmso, dimethyl sulfoxide; Etpyz, 2-ethylpyrazine; Fc, ferrocene; F$_4$dib, 2,3,5,6-tetrafluoro-1,4-diisocyanobenzene; im, imidazole; iqnl, isoquinoline; lut, lutidine; Medib, 2-methyl-1,4-diisocyanobenzene; Me$_2$dib, 2,5-dimethyl-1,4-diisocyanobenzene; Me$_4$dib, 2,3,5,6-tetramethyl-1,4-diisocyanobenzene; Meim, N-methylimidazole; Mepy, methylpyridine; Me$_2$pyNC, 4-isocyano-3,5-dimethylpyridine; Mepyz, 2-methylpyrazine; Me$_2$pyz, 2,6-dimethylpyrazine; Me$_2$pyz, 2,6-dimethylpyrazine; Meqnx, 2-methylquinoxaline; Me$_2$tz, 3,6-dimethyl-s-tetrazine; Nc, naphthalocyanine; npd, 1,5-naphthyridine; Pc, phthalocyanine; pdz, pyridazine; PhCN, benzonitrile; PhNC, isocyanobenzene; Pn, porphyrin; ppd, p-phenylenediamine; ptz, phthalazine; py, pyridine; pypyz, pyrido[2,3-b]pyrazine; pyz, pyrazine; qnl, quinoline; qnz, quinazoline; qnx, quinoxaline; thf, tetrahydrofuran; tri, 1,2,4-triazine; triest, 3-ethoxycarbonyl-1,2,4-triazine; TPP, tetraphenylporphyrin; tz, s-tetrazine

* Corresponding author. Tel.: +61 2 95141035.
E-mail address: andrew.mcdonagh@uts.edu.au (A. McDonagh).

0010-8545/$ – see front matter
doi:10.1016/j.ccr.2006.09.011

3.4. Kinetic studies 1148
3.5. Conduction properties of polymers 1148
4. Applications 1151
4.1. RuPc as thin films 1151
4.1.1. Thin films by evaporation and vacuum deposition 1151
4.1.2. Langmuir–Blodgett thin films 1151
4.1.3. Self-assembled monolayers 1151
4.2. Catalysis 1152
4.2.1. Oxidation catalysts 1152
4.2.2. Reduction catalysts 1153
4.2.3. Hydrogenation and cyclopropanation catalysts 1154
4.3. Photodynamic therapy 1154
4.4. Dye-sensitised solar cells 1154
5. Conclusions 1155
References 1155

Abstract

This article reviews the synthesis of ruthenium phthalocyanine and naphthalocyanine complexes highlighting important advances, and examines their physical properties and applications.

Keywords: Ruthenium; Phthalocyanine; Naphthalocyanine

1. Introduction

Metallophthalocyanine complexes have attracted considerable attention due to their impressive and useful chemical and physical properties [1–4]. The transition metal ruthenium has a rich and varied chemistry [5,6]. It is unsurprising therefore that numerous ruthenium phthalocyanine and naphthalocyanine complexes (Fig. 1) have been reported in the literature. To date, no comprehensive review of these classes of complexes has been published.

This article describes the synthesis of ruthenium phthalocyanine and naphthalocyanine complexes together with a discussion of their properties and applications.

2. Synthesis

2.1. Synthesis of complexes with unsubstituted phthalocyanine macrocycles

2.1.1. Ring-forming syntheses

2.1.1.1. Synthesis by fusion in the absence of solvent. Krueger and Kenney [7] reported the first synthesis of ruthenium phthalocyanine complexes in 1963. Heating 2-cyanobenzamide with $RuCl_3$ (Scheme 1) yielded a "crude PcRu" complex, which was recrystallised from aniline to yield a product reported as [PcRu·6($C_6H_5NH_2$)]. Similarly, recrystallising "crude PcRu" from *o*-toluidine afforded [PcRu·6(*o*-$MeC_6H_4NH_2$)].

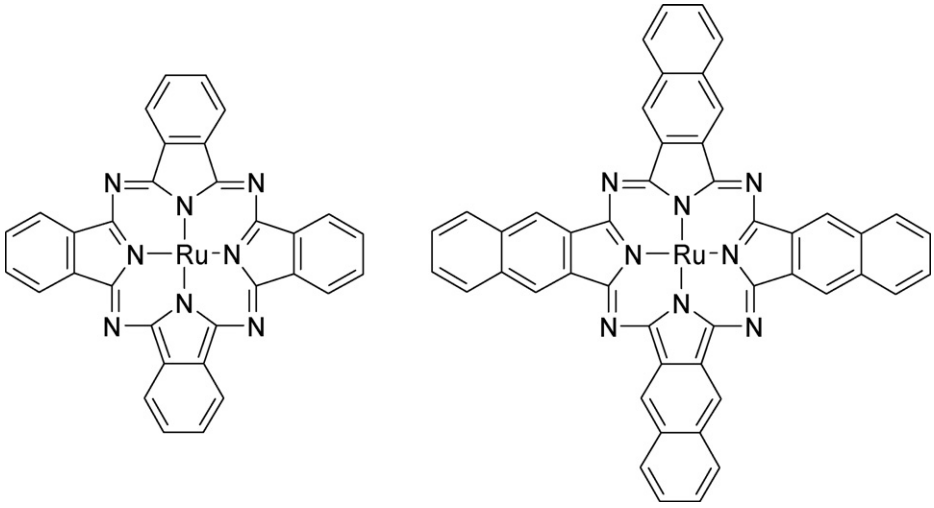

Fig. 1. Left: ruthenium phthalocyanine (PcRu). Right: ruthenium 2,3-naphthalocyanine (2,3-NcRu).

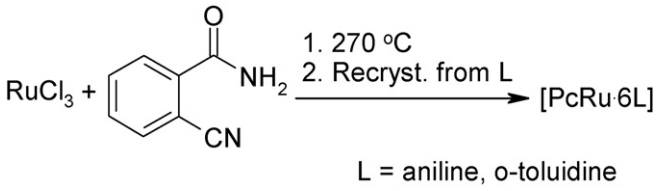

Scheme 1. Reaction of $RuCl_3$ with 2-cyanobenzamide reported by Krueger and Kenney [7].

The "crude PcRu" complex was subsequently reported to be $[PcRu^{III}Cl{\cdot}C_6H_4(CN)(CONH_2)]$ [8]. Similarly prepared from phthalonitrile was a complex reported as $[PcRu^{III}Cl{\cdot}C_6H_4(CN)_2]$ [8,9]. The formation and nature of chlorine-containing species obtained from reactions of $[RuCl_3{\cdot}xH_2O]$ with 2-cyanobenzamide or phthalonitrile have attracted considerable discussion. The preparation of a ring-chlorinated complex, $[Pc(Cl)Ru^{III}Cl]$, from phthalonitrile and $RuCl_3$ was reported [10], however others [11] suggested that $[PcRu^{III}Cl]$ is only a minor product of the reaction of $[RuCl_3{\cdot}xH_2O]$ with phthalonitrile or 2-cyanobenzamide. Boucher and Rivera [12] reported that reacting phthalonitrile with $[RuCl_3{\cdot}xH_2O]$ followed by extraction with pyridine does not form a Ru(III) complex, but rather a Ru(II) complex bearing two axially coordinated pyridine ligands and a monochlorinated phthalocyanine macrocycle. The ^1H NMR spectrum of their diamagnetic complex was reported to be consistent with this formulation. Doeff and Sweigart [13] reacted phthalonitrile with $[RuCl_3{\cdot}3H_2O]$ in air, argon and CO, and with $[Ru_3(CO)_{12}]$, as well as various axial ligands. Using $[RuCl_3{\cdot}3H_2O]$ as starting material, chlorine-containing complexes were obtained. The mass spectrum of one such complex, $[(PcCl)Ru\{P(OBu)_3\}_2]$ contained a major ion cluster corresponding to the molecular ion indicating that chlorine was not present as ionic chloride associated with a trivalent ruthenium ion. When $[Ru_3(CO)_{12}]$ was used as starting material, no chlorinated products were detected. However, where Boucher and Rivera reported clear differences in the ^1H NMR spectra of non-chlorinated and monochlorinated phthalocyanine rings [12], Doeff and Sweigart reported identical ^1H and ^{13}C NMR spectra for the two ring systems. It was later reported [14] that complexes prepared from $[RuCl_3{\cdot}xH_2O]$ by the method of Doeff and Sweigart [13] gave low C, H, N analyses more consistent with 1.5 chlorines/ruthenium but no spectral or kinetic differences compared to non-chlorinated complexes prepared from $[Ru_3(CO)_{12}]$ were observed. A review of ruthenium chemistry [15] states that claims of a ring-chlorinated phthalocyanine complex reported by Boucher and Rivera [12] were incorrect, suggesting that the NMR spectra are more consistent with a mixture of $[PcRu(py)_2]$ and $[PcRu(py)(solvent)]$. Furthermore, there are conflicting reports describing ring-chlorination with reactions performed under an atmosphere of CO [11–13]. The issue of ring chlorination appears yet to be fully resolved.

However, the use of $[Ru_3(CO)_{12}]$ [11,13,14] as a ruthenium source yields complexes free of chlorine, and the use of a solvent such as naphthalene also gives chlorine-free products even when $[RuCl_3{\cdot}3H_2O]$ is used as starting material [12].

More recently, the use of microwave radiation to facilitate ring formation was reported. Phthalonitrile, urea, ammonium chloride, ammonium molybdate and dehydrated $RuCl_3$ were reacted under microwave irradiation to give a crude product, which was extracted with pyridine and purified by column chromatography to afford $[PcRu(py)_2]$ in 60% yield [16]. Under similar conditions using phthalic anhydride and without ammonium molybdate, a slight increase in yield to 65% was reported [17]. Reaction of phthalonitrile and $RuCl_3$ in a modified microwave oven was reported to give [PcRu(Cl)] in 91% yield [18] although limited characterisation data were provided, making this formulation unreliable.

2.1.1.2. Synthesis using solvent. James et al. [19,20] showed that the reaction of $[RuCl_3{\cdot}3H_2O]$ with 2-cyanobenzamide using naphthalene as solvent, followed by Soxhlet extraction of the crude product with L (where L = py, 4-Mepy, 4-Bupy) reliably gave $[PcRuL_2]$ complexes in moderate yields. This synthetic method, with modifications to include a variety of different axial ligands, has been used in numerous subsequent investigations.

Bossard et al. developed a route to ruthenium phthalocyanine complexes (Scheme 2) whereby $[RuCl_3{\cdot}xH_2O]$ is first dehydrated by boiling in pentanol until blue (so-called "ruthenium blue") and subsequently reacted with phthalonitrile, ammonia, and hydroquinone to form the virtually insoluble $[PcRu(NH_3)_2]$, which was purified by washing with solvent [21,22]. Reaction of this complex with benzonitrile afforded $[PcRu(PhCN)_2]$; the labile benzonitrile ligands are readily substituted by other ligands to prepare various PcRu complexes.

Yanagisawa et al. [23] reacted phthalonitrile, $[RuCl_3{\cdot}3H_2O]$ and 4-methylpyridine in 2-ethoxyethanol with a catalytic amount of 1,8-diazabicyclo[5.4.0]undec-7-ene (DBU) to form $[PcRu(4\text{-}Mepy)_2]$ (Scheme 3). This procedure has been used extensively in ring-substituted PcRu syntheses (see Section 2.2). Similarly, Hanack et al. reacted phthalonitrile with DBU and $[Ru_2Cl_3(PEt_2Ph)_6]Cl$ in pentanol affording $[PcRu(PEt_2Ph)_2]$ [24]. Table 1 presents a summary of some unsubstituted ring-forming syntheses.

2.1.1.3. Synthesis using zeolites. The synthesis of ruthenium phthalocyanine inside zeolite supercages has been reported [25–29]. Ruthenium inclusion into the zeolite was achieved by:

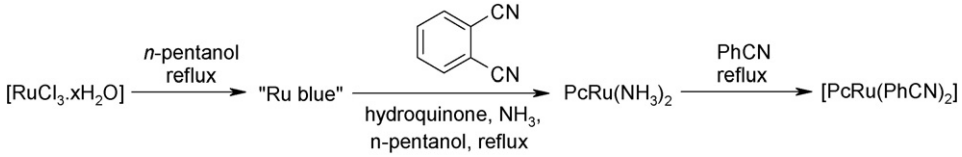

Scheme 2. Synthetic method of Bossard et al. [21,22].

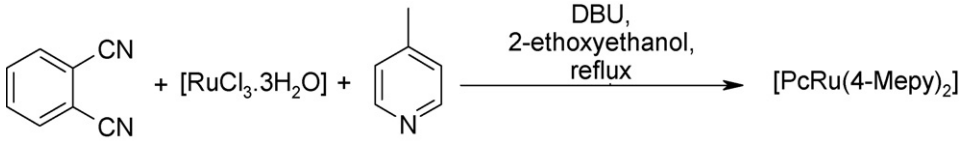

Scheme 3. Synthetic method of Yanagisawa et al. [23].

(a) cation exchange using $[RuNO(NH_3)_4OH]^{2+}$, and (b) introduction of the labile π-complex di(cyclopentadienyl)ruthenium under vacuum. The ruthenium-containing zeolite was subsequently exposed to phthalonitrile vapour under vacuum at 150–270 °C to form an entrapped PcRu complex. The zeolite was dissolved in hot sulfuric acid and the UV–vis spectrum of the resulting solution showed absorption bands indicative of a PcRu complex. X-ray photoelectron spectroscopy data indicated conversion of di(cyclopentadienyl)ruthenium to ruthenium phthalocyanine of up to 89%. Zeolite-encapsulated ruthenium phthalocyanine was also prepared by the cation exchange method whereby the zeolite was stirred in a solution of $[RuCl_2(dmso)_4]$ and then heated with phthalonitrile in nitrobenzene [30]. In the above reports, although sufficient data was obtained to identify the presence of ruthenium phthalocyanine complexes, due to the difficulties in identifying species

Table 1
Summary of unsubstituted macrocycle ring-forming synthetic procedures

Reactants	Reaction conditions	Products	Notes	References
2-Cyanobenzamide, $RuCl_3$	270 °C, 2 h	"crude PcRu"	Limited characterization data. Product later reported as $[PcRu^{III}Cl{\cdot}C_6H_4(CN)(CONH_2)]$ [8] but subsequently $PcRu^{II}$ reported to be the predominant species [11]	[7]
(a) 2-Cyanobenzamide, $RuCl_3{\cdot}3H_2O$ (b) 4-Rpy	(a) 290 °C, naphthalene, 1 h (b) Soxhlet extraction with 4-Rpy	$[PcRu(4\text{-}Rpy)_2]$	R = H, Me, *t*Bu	[19]
Phthalonitrile, $RuCl_3{\cdot}xH_2O$	290 °C, 2 h	$[PcRu^{III}Cl{\cdot}C_6H_4(CN)_2]$	Also reported to give $[Pc(Cl)Ru^{III}Cl]$ [10]. Main product more likely to be a $PcRu^{II}$ species [11]. Ring-chlorinated products also reported [12]	[8,9]
(a) Phthalonitrile, $RuCl_3{\cdot}3H_2O$ (b) py	(a) 250 °C, CO atmosphere, 4 h (b) py, reflux	[PcRu(CO)(py)]	Product reported as $[Pc(Cl)Ru(py)_2]$ elsewhere [13]	[11]
(a) Phthalonitrile, $RuCl_3{\cdot}xH_2O$ (b) py	(a) 280 °C, (b) Soxhlet extraction with py	$[Pc(Cl)Ru^{II}(py)_2].4py$	Product suggested to be a mixture of $[PcRu(py)_2]$ and [PcRu(py)(solvent)] [15]	[12]
(a) Phthalonitrile, $Ru_3(CO)_{12}$ (b) py	(a) 250 °C, (b) py, 150 °C	[PcRu(CO)(py)]	Debate over the nature of the intermediate formed prior to reaction with py [11,13,14] Replacing py with phosphines in Step (b) gives $[PcRuL_2]$ where $L = PBu_3$, $P(OBu)_3$ [13]	[11]
(a) Phthalonitrile, urea, $RuCl_3$ (b) py	(a) Microwave irradiation, NH_4Cl, $(NH_4)_2MoO_4$, 5 min. (b) Soxhlet extraction with py	$[PcRu(py)_2]$		[16]
(a) Phthalic anhydride, urea, Ru (b) py	(a) Microwave irradiation, NH_4Cl, 6 min. (b) Soxhlet extraction py	$[PcRu(py)_2]$	Ruthenium source not specified	[17]
Phthalonitrile, $RuCl_3{\cdot}3H_2O$,	Microwave irradiation, 5–15 min	Pc(Cl)Ru	Very limited characterisation data provided, formulation possibly unreliable	[18]
(a) $RuCl_3{\cdot}3H_2O$ (b) Phthalonitrile, NH_3, hydroquinone	(a) $RuCl_3.3H_2O$ converted to "ruthenium blue" in pentanol (b) Pentanol, reflux, 72 h	$[PcRu(NH_3)_2]$		[21,22]
Phthalonitrile, $RuCl_3{\cdot}3H_2O$, 4-Mepy	2-Ethoxyethanol, DBU, reflux, 8 h	$[PcRu(4\text{-}Mepy)_2]$		[23]
Phthalonitrile, $[Ru_2Cl_3(PEt_2Ph)_6]Cl$	Pentanol, DBU, reflux, 8 h	$[PcRu(PEt_2Ph)_2]$		[24]

formed inside zeolite cages, definitive assignments of molecular structures were not given.

2.1.2. Synthesis by incorporation of Ru into the phthalocyanine macrocycle

There are numerous reports describing how metal centres may be incorporated into the Pc macrocycle [1]. Direct incorporation of Ru(II) was achieved by reaction of H_2Pc with $[Ru_3(CO)_{12}]$ to give a product tentatively described as [PcRu(CO)] [19]. Ruthenium incorporation using M_2Pc (where M = H, Li, Na) and various ruthenium sources resulted in only a small amount of metallation [19,20].

2.1.3. Synthesis involving axial ligand substitution

2.1.3.1. Synthesis from "crude PcRu". As previously mentioned, the ring-forming reaction between $[RuCl_3{\cdot}xH_2O]$ and 2-cyanobenzamide or phthalonitrile yields initially a "crude PcRu" complex [7,19]. Ligand substitution reactions have been performed using this crude reaction product followed by purification of the resultant complexes.

The "crude PcRu" may be reacted with dmso to form $[RuPc(dmso)_2]$ [20,31,32]. This useful complex has been used to prepare pure ruthenium phthalocyanine as well as other complexes by dmso ligand exchange. Reacting "crude PcRu" with dmf gives the carbonyl complex [PcRu(CO)dmf] [19,20]. "Crude PcRu" was used to prepare the first reported complexes with phosphine or phosphite ligands, $[PcRu(PBu_3)_2]$ and $[PcRu\{P(OBu_3)\}_2]$ as well as complexes with *N*-methylimidazole and pyridine ligands [13]. [PcRu(4-carboxypyridine)$_2$] was prepared from "crude PcRu" with 4-pyridinecarboxylic acid [23]. $K_2[PcRu(CN)_2]{\cdot}3H_2O$ was synthesised from "crude PcRu" and KCN in 66% yield although reacting $[PcRu(dmso)_2]{\cdot}2dmso$ with KCN gave the desired complex with an increased yield of 80% [33].

2.1.3.2. Synthesis from pure ruthenium phthalocyanine. The synthesis of analytically pure ruthenium phthalocyanine was first reported by Kobel and Hanack in 1986 [32]. Heating $[PcRu(dmso)_2]{\cdot}2dmso$ to 330 °C *in vacuo* displaced dmso ligands to afford pure ruthenium phthalocyanine in quantitative yield. Alternative routes into pure ruthenium phthalocyanine by sublimation of "crude PcRu" [34], and by thermal displacement of pyridine ligands [34,35] and isoquinoline ligands [35,36] were subsequently reported. Pure ruthenium phthalocyanine exists as a dimer $[(PcRu)_2]$ [37]; a discussion of the structure may be found in Section 3.

Ruthenium phthalocyanine reacts with pyridine, methyl-, fluoro-, and chloro-pyridines to form the corresponding bis-axially substituted complexes [38,39]. Reaction of ruthenium phthalocyanine with isocyanide ligands forms $[PcRu(CNR)_2]$ complexes where R = *t*-Bu, cyclohexyl, benzyl, phenyl and 2,6-dimethylphenyl groups [40]. By using a large excess of the coordinating ligand, the monomeric complexes $[PcRu(dib)_2]$ and $[PcRu(Me_4dib)_2]$ were prepared from the potentially bridging ligands 1,4-diisocyanobenzene (dib) and 2,3,5,6-tetramethyl-1,4-diisocyanobenzene (Me_4dib) [32,41]. Other monomeric complexes of the potentially bridging ligands pyrazine (including substituted pyrazines), 4,4-bipyridine, pyridazine, 3,6-dimethylpyridazine, pyrimidine, *s*-tetrazine, and 3,6-dimethyl-*s*-tetrazine were also prepared by reaction of the ligand with ruthenium phthalocyanine [32,42,43]. Sterically hindered pyrazine derivatives, e.g. 2,5-dimethylpyrazine, did not form complexes and where only one coordination site was hindered, e.g. 2-substituted pyrazines, coordination occurred exclusively through the non-hindered nitrogen of the ligand [32]. Similarly, complexes with azanaphthalene ligands such as quinoxaline, 2-methylquinoxaline, quinazoline, phthalazine, quinoline, pyrido[2,3-*b*]pyrazine, pteridine, isoquinoline, and 1,5-napthyridine have been reported [44]. NMR data showed that coordination occurs at the sterically less hindered isoquinoline-like N atom.

Alkynyl PcRu complexes, $Li[PcRuC{\equiv}CR]{\cdot}x$thf (where R = phenyl or t-butyl groups) are formed by treatment of ruthenium phthalocyanine with the corresponding lithium acetylide compounds [45]. Also prepared from ruthenium phthalocyanine was the amine complex [PcRu(*n*-butylamine)$_2$] [46], and the phosphane complexes $[PcRu(PEt_2Ph)_2]$ and $[PcRu(PPh_3)_2]$ [24].

2.1.3.3. Ligand exchange reactions. Axial ligand exchange, as shown in Scheme 4, has been shown to proceed readily in a number of examples. Treatment of solutions of $[PcRuL_2]$ (where

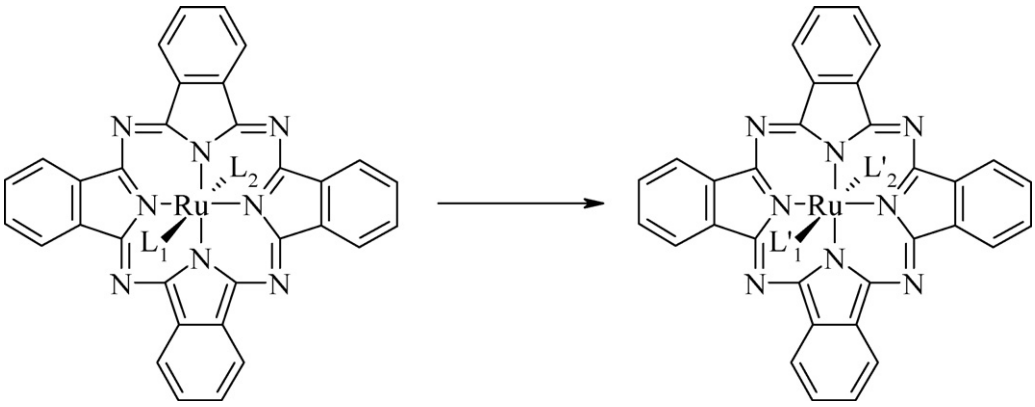

Scheme 4. Axial ligand exchange reactions.

L = py, 4-Mepy, 4-*t*-Bupy, dmso, MeCN) with CO gives the complexes [PcRu(CO)L] [19,20]. Reacting [PcRu(CO)L] (where L = py, 4-Mepy, 4-Bupy, dmf) with excess L under photolysis conditions gives [PcRuL$_2$] [19], and reacting [PcRu(CO)L] with L′ yields [PcRuL$_2$′] (where L and L′ are, respectively, dmso and py, py and MeCN, dmso and MeCN) [19,20]. Substitution of pyridine ligands in [PcRu(py)$_2$] by MeCN [20] and triphenylphosphine [12] has also been reported. Similarly, reacting [PcRu(4-Mepy)$_2$] with pyridine ligands bearing phosphonate groups gave a mixture of [PcRu(4-Mepy)$_2$], [PcRu(4-Mepy)L] and [PcRuL$_2$] where L is the pyridine 4-phosphonate ligand [47]. The complexes were separated using column chromatography. The dmso ligands in [PcRu(dmso)$_2$] may be readily substituted with dmf, im, py, MeCN and CN^- ligands [19,20,33].

Reacting [PcRu(NH$_3$)$_2$] with benzonitrile affords [PcRu(PhCN)$_2$] [21,22]. The labile benzonitrile ligands have been substituted by the ligands $Ph_2P(3\text{-}C_6H_4SO_3^-)$ [21,22], $3\text{-}pySO_3^-$ [21], 1,4-diisocyanobenzene [48], 4-pyCHO [49], and 4,4′-bpy [50]. From the benzylisocyanide complex [PcRu(BzNC)$_2$], one isocyanide ligand may be substituted by Meim or *t*-Bupy to form the mixed ligand complexes [PcRu(BzNC)L] (L = Meim or *t*-Bupy) [14].

Homborg et al. report a number of PcRu halogen complexes with the metal centre and Pc macrocycle in various oxidation states, which are indicated below for clarity (see Section 3.2 for a discussion of the oxidation states of PcRu complexes.). From H[$Pc^{2-}Ru^{III}Cl_2$] was obtained (*n*-Bu$_4$N)[$Pc^{2-}Ru^{III}Cl_2$] by the addition of (*n*-Bu$_4$N)Cl [51]. Similarly, from H[$Pc^{2-}Ru^{III}Br_2$] was obtained (*n*-Bu$_4$N)[$Pc^{2-}Ru^{III}Br_2$] [52]. Interestingly, these complexes have Ru^{III} metal centres, an oxidation state infrequently reported for PcRu complexes.

Reaction of [$Pc^{2-}Ru^{II}(py)_2$] with (*n*-Bu$_4$N)X (where X = Br or Cl) gave (*n*-Bu$_4$N)$_2$[$Pc^{2-}Ru^{II}(X)_2$] [53]. Reacting (*n*-Bu$_4$N)$_2$[$Pc^{2-}Ru^{II}(X)_2$] (X = CN, NCO, NCS, N_3, NO_2) with pyridine forms the mixed ligand complexes (*n*-Bu$_4$N)[$Pc^{2-}Ru^{II}$(X)py] [54].

Reduction of (*n*-Bu$_4$N)[$Pc^{2-}Ru^{III}(OH)_2$] with CO gives [$Pc^{2-}Ru^{II}(H_2O)$(CO)], which with excess (*n*-Bu$_4$N)X (X = Cl, Br, I, NCO, NCS, N_3) yields (*n*-Bu$_4$N)[$Pc^{2-}Ru^{II}$X(CO)] [55]. Also, reaction of H[$Pc^{2-}Ru^{III}Cl_2$] with (*n*-Bu$_4$N)NO_2 reduces the ruthenium metal centre to form (*n*-Bu$_4$N)$_2$[$Pc^{2-}Ru^{II}(NO_2)_2$] [56].

Oxidation of (*n*-Bu$_4$N)[$Pc^{2-}Ru^{II}$X(CO)] (X = Cl, Br) with halogen or benzoyl peroxide gives [$Pc^{-}Ru^{II}$X(CO)] [57] and oxidation of (*n*-Bu$_4$N)[$Pc^{2-}Ru^{III}X_2$] (X = Cl or Br) with additional halogen, X, gives [$Pc^{-}Ru^{III}X_2$] [58]. Similarly, reacting (*n*-Bu$_4$N)[$Pc^{2-}Ru^{III}(OH)_2$] with iodine forms [$Pc^{-}Ru^{III}I_2$] [58].

Acidification of (*n*-Bu$_4$N)$_2$[$Pc^{2-}Ru^{II}(NO_2)_2$] with the appropriate mineral acids or ammonium salts gives the nitrosyl complexes [$Pc^{2-}Ru^{II}$X(NO)] (X = F, Cl, Br, I, CN, NCO, NCS, NCSe, N_3, NO_2) [59].

2.1.4. Dimeric and polymeric complexes

The simplest dimer is that of pure ruthenium phthalocyanine i.e., [(PcRu)$_2$]; its synthesis is described in the previous section. The nitrido-bridged dimer, [(PcRu)$_2$N], was prepared by reacting ruthenium phthalocyanine or [PcRu(py)$_2$] with NaN_3 in α-chloronaphthalene [34]. A bimetallic μ-nitrido dimer, [(TPP)Fe–N–RuPc] where TPP is tetraphenylporphyrin, was prepared by heating a suspension of [(TPP)FeN_3] and [(PcRu)$_2$] in xylene [60]. The complex was oxidised with I_2 affording [(TPP)Fe–N–PcRu]$^+$ with I_5^- as the counter anion. Reduction of this species with $NaBH_4$ re-formed the starting dimer.

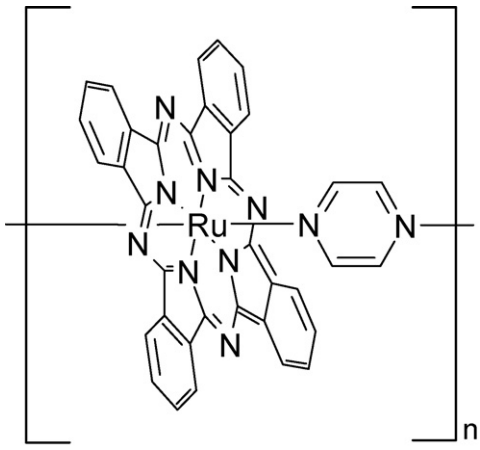

Fig. 2. The [PcRu(pyz)]$_n$ polymer reported by Hanack et al. [63].

The μ-carbido complex [{PcRu}$_2$(μ-C)] was prepared in a "one-pot" synthesis [61,62]. H[$RuCl_2$Pc] was reduced by potassium hydroxide and then oxidised with dichlorocarbene (produced *in situ* from chloroform and potassium hydroxide) to form the dichlorocarbene complex [PcRu(CCl_2)]. Condensation yielded the crude μ-carbido complex, which can be isolated as the pyridine adduct [{RuPc(py)}$_2$(μ-C)]. The pyridine ligands may be subsequently removed by heating under vacuum.

Hanack et al. reported the first axially bridged ruthenium phthalocyanine polymer, [PcRu(pyz)]$_n$ [63]. It was prepared by heating the monomer [PcRu(pyz)$_2$] until one pyrazine ligand dissociates (determined by thermogravimetry/differential thermal analysis), yielding the polymer shown in Fig. 2 [32,64].

This procedure was also applied to the preparation of [PcRu(4,4′-bpy)]$_n$ [32], [PcRu(Me_4dib)]$_n$ and [PcRu(Cl_4dib)]$_n$ [41], and [PcRu(bpyac)]$_n$ [64]. [PcRu(Me_4dib)]$_n$ and [PcRu(Cl_4dib)]$_n$ were formed by stirring solutions of the corresponding monomers at room temperature for 2 days [41]. Axially bridged polymers can also be prepared by the reaction of an appropriate bidentate ligand with [PcRu]. The polymer [PcRu(dib)]$_n$ was prepared by refluxing ruthenium phthalocyanine with a 1:1.1 molar ratio of diisocyanobenzene in acetone [32,65]. Similarly prepared were the polymers [PcRu(Me_4dib)]$_n$ and [PcRu(Cl_4dib)]$_n$ [41], [PcRu(tz)]$_n$ [42,65,66], [PcRu(Me_2tz)]$_n$ [43], [PcRu(ppd)]$_n$, [PcRu(daf)]$_n$, and [PcRu(apy)]$_n$ [67]. Bridging ligands bearing alkyl sidechains such as 1,4-diisocyano-2,5-di-*t*-butylbenzene, have been reacted with ruthenium phthalocyanine in order to produce more soluble polymers [68,69].

Capobianchi et al. found that [(PcRu)$_2$] reacts with O_2 in 1-chloronaphthalene, benzene or toluene to form the oxygen-containing polymer HO–[(Pc)RuO]$_n$–H (average $n = 11$), which consists of (Pc)Ru^{IV}O fragments [70].

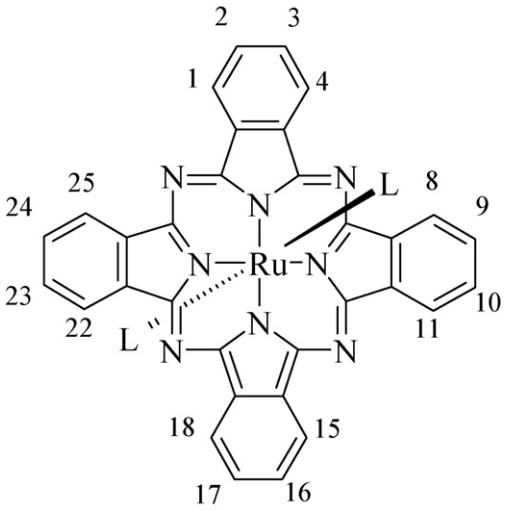

Fig. 3. Numbering scheme for Pc ring positions.

The conduction properties of the polymers described above are discussed in Section 3.5.

2.2. Synthesis of complexes with substituted phthalocyanine macrocycles

This section describes the synthesis of complexes substituted about the macrocyclic ring (Fig. 3). Tetra-substituted complexes, where the four substituents are identical, may exist as four possible positional isomers. Fig. 4 shows the isomers that can arise from substitution of the outermost carbon atoms of the macrocycle. In subsequent discussions, we will refer to tetra-substituted complexes using the designation of the isomer shown in Fig. 4A only, i.e. 2,9,16,23-, although the other isomers are assumed to be present as a mixture. We note that complexes bearing either one axial ligand or two different axial ligands with tetra-substitution of the type shown in Fig. 4A or B can exist as enantiomers [71] although no ruthenium phthalocyanine complexes have been resolved. Octa-substituted complexes with identical peripheral substituents in either the 1,4,8,11,15,18,22,25 or 2,3,9,10,16,17,23,24 positions do not have positional isomers, nor do the hexadeca-substituted complexes bearing identical substituents.

2.2.1. Substituted ring-forming syntheses

The first reported ring-substituted ruthenium phthalocyanine complex was [{$(NaSO_3)_4$Pc}Ru$(OH)_2$] (the positions of the sulfonate groups were not reported) [72]. Reaction of potassium oxochlororuthenate(IV), ammonium sulfophthalate, and urea at 230 °C yielded [{$(NaSO_3)_4$Pc}Ru$(OH)_2$]·$4H_2O$ together with a bridged dimer reported as [{$(NaSO_3)_4$PcRuOH}$_2$O]·$8H_2O$. Similarly, [{2,9,16,23-$(NaSO_3)_4$Pc}Ru] was prepared by reaction of sodium 4-sulfophthalate, urea, and [$RuCl_2$(dmso)$_4$] with ammonium chloride and ammonium molybdate as catalysts [30], or by reacting sodium 4-sulfophthalate with [$RuCl_3 \cdot 3H_2O$] in the presence of urea [73,74]. It is suggested [73,74] that water molecules occupy the axial positions in this complex.

Hanack et al. prepared [{2,9,16,23-(*t*Bu)$_4$Pc}Ru] by reaction of 4(5)-*t*-butyl-*o*-cyanobenzamide with $RuCl_3$ in naphthalene, however a pure product was not obtained [38,75]. Reacting 1,3-diimino-5-*t*-butyl-1,3-dihydroisoindoline with [$RuCl_3 \cdot xH_2O$] in the presence of N-donor ligands afforded pure [{2,9,16,23-(*t*Bu)$_4$Pc}RuL$_2$] after chromatography (Scheme 5) [76,77]. In ammonia-saturated 2-ethoxyethanol the reaction affords [{2,9,16,23-(*t*Bu)$_4$Pc}Ru$(NH_3)_2$] [78].

Reaction of 4-*t*-butylphthalonitrile with [$RuCl_3 \cdot 3H_2O$] in 2-ethoxyethanol and DBU with 3-chloropyridine gave [{2,9,16,23-(*t*Bu)$_4$Pc}Ru(3-Clpy)$_2$] [78].

[(2,9,16,23-R$_4$Pc)Ru] (where R = Et, *t*Bu) was rapidly prepared from the reaction of the corresponding phthalonitrile with [$RuCl_3 \cdot 3H_2O$] and DBU catalyst under autoclave conditions [69]. The soluble crude product was purified by column chromatography. The characterisation and purity of the product [{2,9,16,23-(*t*Bu$_4$)Pc}Ru], was questioned by Dudnik et al. Under the same reaction conditions, they observed a complex bearing a carbonyl ligand, as evidenced by the IR spectrum, indicating the product to be [{2,9,16,23-(*t*Bu)$_4$Pc}Ru(CO)] [79]. Dudnik et al. attempted to prepare [{2,9,16,23-(*t*Bu)$_4$Pc}Ru] by the reaction of 4-*t*-butylphthalonitrile with [$RuCl_3 \cdot 3H_2O$] in isoamyl alcohol with DBU (at ambient pressure). Again they found that the monocarbonyl complex [{2,9,16,23-(*t*Bu)$_4$Pc}Ru(CO)] formed [79]. Yields were significantly reduced using the higher boiling point solvent *o*-dichlorobenzene, presumably due to the absence of solvent hydroxy groups. The reaction in quinoline yielded two products; the major product was [{2,9,16,23-

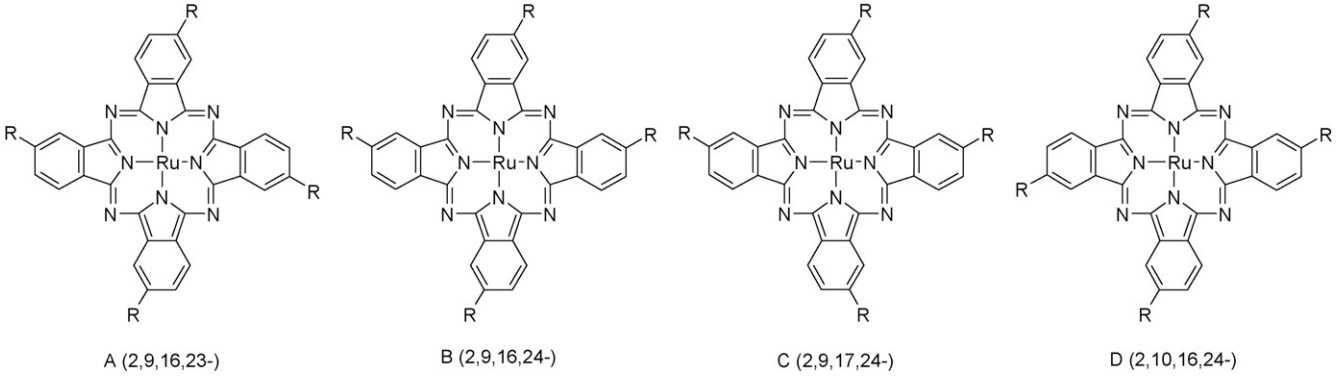

Fig. 4. Positional isomers of tetra-substituted ruthenium phthalocyanine.

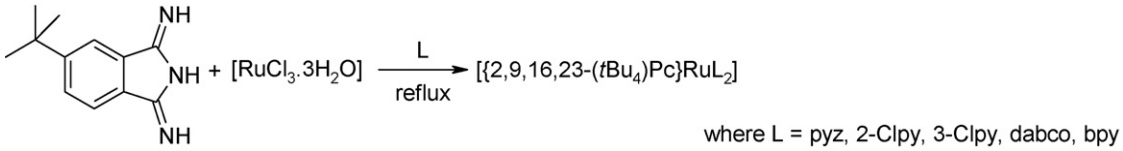

Scheme 5. Synthetic method of Hanack et al. [76,77].

(tBu)$_4$Pc}Ru(iqnl)$_2$], the isoquinoline being an impurity in the quinoline (as previously observed by Hanack et al. [36]), and the minor product was a dimeric species [({2,9,16,23-(tBu)$_4$Pc}Ru(iqnl))$_2$], with a Ru = Ru bond indicated by Raman spectroscopy.

The trimethylsilyl-substituted complex [{2,9,16,23-(Me$_3$Si)$_4$Pc}Ru(3-Clpy)$_2$] was prepared by the reaction of 1,2-dicyano-4-trimethylsilylbenzene with [RuCl$_3$·xH$_2$O] and 3-chloropyridine [80]. When the reaction was left in refluxing solvent for extended periods (5 days) the trisubstituted [{(Me$_3$Si)$_3$Pc}Ru(3-Clpy)$_2$] and disubstituted [{(Me$_3$Si)$_2$Pc}Ru(3-Clpy)$_2$] compounds were also formed.

The octakis(pentyloxy) substituted complex, [{(2,3,9,10,16,17,23,24-C$_5$H$_{11}$O)$_8$Pc}Ru(3-Clpy)$_2$], was prepared following previously reported reaction conditions [78] but starting with 4,5-bis(pentyloxy)phthalonitrile [81]. Using 3,6-dipentyloxyphthalonitrile under the same conditions afforded [{(1,4,8,11,15,18,22,25-C$_5$H$_{11}$O)$_8$Pc}Ru(3-Clpy)$_2$] [39]. 2,3,9,10,16,17,23,24-octakispentyloxy-substituted complexes were prepared using the same method [23]. The reaction proceeded smoothly with 4-methylpyridine axial ligands but with methyl isonicotinate, two products were obtained in very low yields. *Trans*-esterification with the solvent 2-ethoxyethanol gave the bis[4-(2-ethoxy)ethyloxycarbonylpyridine] complex as well as an unsymmetrical complex with 4-(2-ethoxy)ethyloxycarbonylpyridine and 4-pyridinecarboxylic acid as ligands. Using 4-pyridinecarboxylic acid as the axial ligand, the latter complex was obtained exclusively although in low yield (2%).

Gorbunova et al. [82–84] found that reacting a melt of dicyano-benzo-15-crown-5 with either [RuCl$_3$·3H$_2$O], [Ru$_3$(CO)$_{12}$], [Ru(dmso)$_4$Cl$_2$], or [Ru$_2$(OAc)$_4$Cl]$_n$ yielded [{(15-crown-5)$_4$Pc}Ru(CO)(MeOH)] (the methanol coordinating during chromatography), with the best yields obtained from [Ru$_3$(CO)$_{12}$]. Synthesis using pyridine as solvent failed to yield the desired complex [84], presumably due to the low boiling point of pyridine, but the reaction in quinoline gave [(15-crown-5)$_4$PcRu(iqnl)$_2$].

Hexadecaalkyl-substituted ruthenium phthalocyanine complexes were prepared from 1,2-dicyano-3,6-diheptyl-4,5-dimethylbenzene following previously reported reaction conditions [78], affording [{(1,4,8,11,15,18,22,25-C$_7$H$_{15}$)$_8$(2,3,9,10,16,17,23,24-CH$_3$)$_8$Pc}Ru(3-Clpy)$_2$] in low yield, presumably due to the steric effects of the alkyl substituents [85]. Hexadecafluorophthalocyanine was prepared by the reaction of tetrafluorophthalonitrile and [Ru$_3$(CO)$_{12}$] in 1-chloronaphthalene [86,87], although in a subsequent synthesis using [Ru^{III}(NH$_3$)$_5$I]I$_2$ as a ruthenium source the presence of solvent was found to significantly lower yields [88]. Accordingly, hexadecafluoro- and hexadecachlorophthalocyanine complexes were prepared from a melt of the tetrahalophthalonitrile with [Ru^{III}(NH$_3$)$_5$I]I$_2$ in yields of 40% [88]. The use of [Ru^{III}(NH$_3$)$_5$Cl]Cl$_2$ as a metal source gave lower yields, presumably due to the greater reducing power of iodide aiding the generation of Ru^{II}. Unlike dimeric [(PcRu)$_2$], [F$_{16}$PcRu] and [Cl$_{16}$PcRu] were shown to be monomeric species [88].

Unsymmetrical peripherally substituted complexes were prepared using a 4:1 ratio of 4,5-dipentoxyphthalonitrile and 4,5-[(4-ethoxycarbonyl)phenoxy]phthalonitrile (Scheme 6) [89]. *Trans*-esterification of the ethyl-ester with the solvent gave the corresponding 2-ethoxyethyl ester [{2,3,9,10,16,17-(pentoxy)$_6$-23,24-{(4-pentoxycarbonyl)phenoxy}$_2$Pc}Ru(4-mepy)$_2$]. Hydrolysis of the ester groups afforded the corresponding complex bearing two carboxylic acid groups. Table 2 presents a summary of some substituted ring-forming syntheses.

2.2.2. Synthesis involving zeolites and molecular sieves

Zeolite-encapsulated [(F$_{16}$Pc)Ru] was prepared by synthesising the zeolite around the [(F$_{16}$Pc)Ru] [86,87], giving an encapsulation efficiency of roughly 25%. Methods for preparing molecular sieve encased [(F$_{16}$Pc)Ru] include [90]; (1) ship-in-a-bottle (treatment of molecular sieves with [Ru$_3$CO$_{12}$] and tetrafluorophthalocyanine), (2) molecular sieve synthesis method (addition of [(F$_{16}$Pc)Ru] to the synthesis mixture of the molecular sieves), and (3) grafting (functionalizing the molecular sieve wall with aminopropyltriethoxysilane to give a functional amino group for coordination to [(F$_{16}$Pc)Ru]). For the products of methods (1) and (2), [(F$_{16}$Pc)Ru] was readily washed from the molecular sieve if the pore size was too large (>2 nm). For molecular sieves that retained the [(F$_{16}$Pc)Ru] only low complex loading was observed. Method (3) resulted in a high loading of [(F$_{16}$Pc)Ru] to the molecular sieve wall which was resistant to washing.

2.2.3. Synthesis by incorporation of Ru into a substituted macrocycle

Pure [{2,3,9,10,16,17,23,24-(C$_5$H$_{11}$O)$_8$Pc}Ru] was prepared by reaction of (C$_5$H$_{11}$O)$_8$PcH$_2$ with [RuCl$_3$·xH$_2$O] in 2-ethoxyethanol [35]. Interestingly, 6 years later the same authors reported that only an impure product was obtained under these reaction conditions [81]. The metal exchange reaction between [{2,3,9,10,16,17,23,24-(C$_5$H$_{11}$O)$_8$Pc}Li$_2$] and [RuCl$_3$·3H$_2$O] afforded the carbonyl complex [{2,3,9,10,16,17,23,24-(C$_5$H$_{11}$O)$_8$Pc}Ru(CO)] [35,81]. Similarly, metal insertion into [2,3,9,10,16,17,23,24-(2-Et-hexO)$_8$PcLi$_2$] gave the corresponding mono-carbonyl [81].

[{1,4,8,11,15,18,22,25-(OBu)$_8$Pc}Ru(CO)(py)] was prepared by metal insertion synthesis using [{1,4,8,11,15,18,22,25-(OBu)$_8$Pc}H$_2$] with [Ru$_3$(CO)$_{12}$] in pyridine [91]. The metal

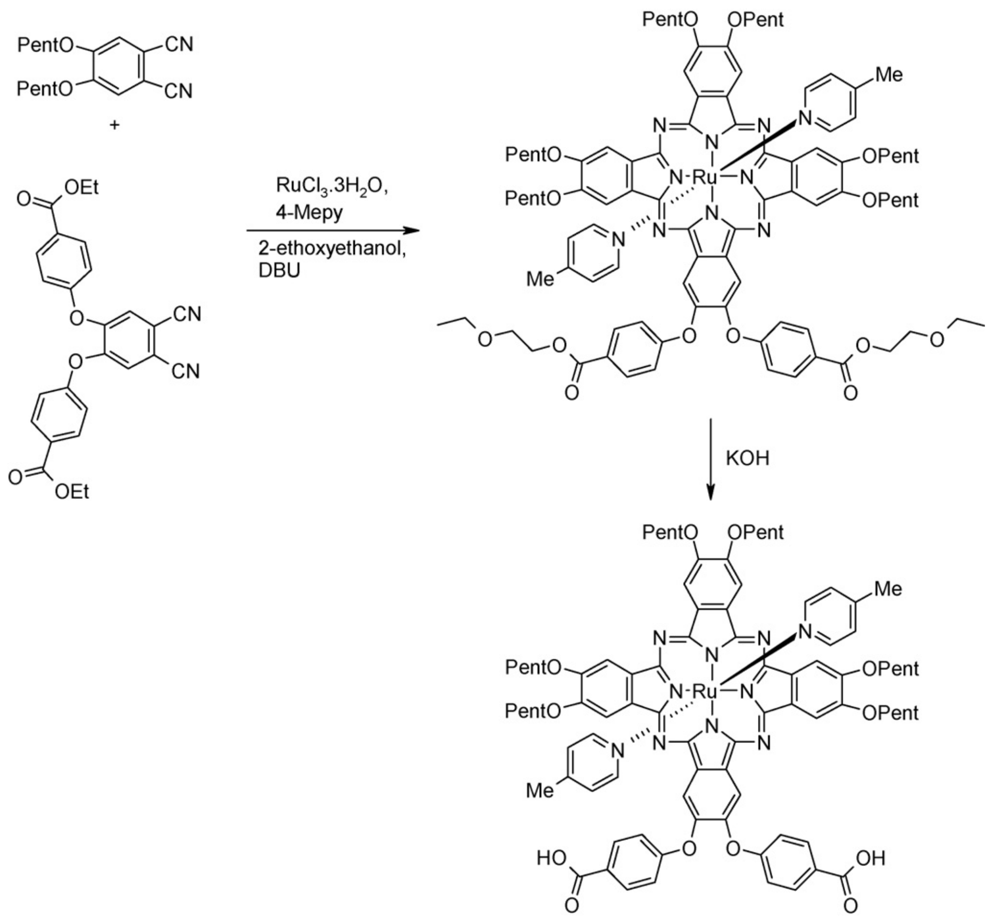

Scheme 6. Synthesis of unsymmetrical peripherally substituted complexes [89].

insertion reaction of [{1,4,8,11,15,18,22,25-(*n*-octyl)$_8$Pc}H_2] and [$Ru_3(CO)_{12}$] in benzonitrile forms a mixture of the mono-carbonyl and bis-benzonitrile complexes [92,93]. Refluxing in benzonitrile for extended periods yields exclusively the bis-benzonitrile complex while reduced reaction times or treatment of the reaction mixture with CO gives predominantly the mono-carbonyl complex. A similar result was reported for the preparation of [{1,4,8,11,15,18,22,25-(*n*-decyl)$_8$Pc}Ru(CO)] [93].

2.2.4. Synthesis involving axial ligand substitution

2.2.4.1. Synthesis from crude [(R_xPc)Ru]. Crude [{2,9,16,23-(*t*-Bu_4)Pc}Ru] was utilized to prepare a series of complexes with pyridine and methyl-substituted pyridine axial ligands [38]. The crude [{2,9,16,23-(*t*-Bu_4)Pc}Ru] was heated in molten ligand to afford pure [{2,9,16,23-(*t*-Bu_4)Pc}RuL_2] after chromatography (where L = py, 2-Mepy, 3-Mepy, 4-Mepy, 2,5-lut, 2,6-lut). Crude [{2,9,16,23-(*t*-Bu_4)Pc}Ru] was also used in the preparation of axially bridged polymers [75] (see Section 2.2.5).

2.2.4.2. Synthesis from pure [(R_xPc)Ru]. The synthesis of pure [{2,9,16,23-(*t*Bu)$_4$Pc}Ru] was first reported by Hanack et al. Initial attempts to thermally decompose [{2,9,16,23-(*t*Bu)$_4$Pc}RuL_2] (where L = py, 2-Mepy, 3-Mepy, 4-Mepy, 2,5-lut, 2,6-lut) failed [38]. However, with 3-chloropyridine or ammonia as axial ligands, heating the complex at 280 °C gave quantitative yields of [{2,9,16,23-(*t*Bu)$_4$Pc}Ru] [78]. This complex was also prepared by the thermal decomposition of [{2,9,16,23-(*t*Bu)$_4$Pc}Ru(iqnl)$_2$] under high vacuum [79] and from 4-*t*-butylphthalonitrile under autoclave conditions followed by column chromatography [69], however the characterisation and purity of the product were later questioned (see Section 2.2.1).

Heating pure [(2,9,16,23-Et_4Pc)Ru] (prepared from 4-ethylphthalonitrile under autoclave conditions) in *t*-butyl-isocyanide, pyridine and pyrazine afforded the corresponding bis-axially coordinated complex [69].

3-Chloropyridine was employed as an axial ligand in the synthesis of octa-alkoxy substituted complexes. [{2,3,9,10,16,17,23,24-($C_5H_{11}O$)$_8$Pc}Ru(3-Clpy)$_2$] was heated to 240 °C under vacuum, giving quantitative yields of [{2,3,9,10,16,17,23,24-($C_5H_{11}O$)$_8$Pc}Ru] [81], which was also prepared by metal insertion (see Section 2.2.3). [{2,3,9,10,16,17,23,24-($C_5H_{11}O$)$_8$Pc}Ru] reacts with *t*-butylisocyanide to give the corresponding axially coordinated product [35].

Ruthenium tetra(trimethylsilyl)phthalocyanine, [{2,9,16,23-(Me_3Si)$_4$Pc}Ru], was also prepared by thermolysis of the 3-chloropyridine adduct [80]. The reaction of [{2,9,16,23-

Table 2
Summary of substituted macrocycle ring-forming synthetic procedures

Reactants	Reaction conditions	Products	Notes	References
Ammonium sulfophthalate, potassium chlororuthenate, urea	210–230 °C, 8 h	[{$(NaSO_3)_4$Pc}Ru$(OH)_2$]·$4H_2O$, [{$(NaSO_3)_4$PcRuOH}$_2$O]·$8H_2O$		[72]
Sodium 4-sulfophthalate, [$RuCl_2$(dmso)$_4$], urea	180 °C, NH_4Cl, $(NH_4)_2MoO_4$	[{2,9,16,23-$(NaSO_3)_4$Pc}Ru]		[30]
Sodium 4-sulfophthalate, $RuCl_3.3H_2O$, urea,	Nitrobenzene, NH_4Cl, $(NH_4)_2MoO_4$, 180 °C,	[{2,9,16,23-$(NaSO_3)_4$Pc}Ru]		[73,74]
4(5)-*t*-Butyl-*o*-cyanobenzamide, $RuCl_3$	Naphthalene, 290 °C, 30 min	[{2,9,16,23-(*t*Bu)$_4$Pc}Ru]	Impure product obtained.	[38,75]
1,3-Diimino-5-*t*-butyl-1,3-dihydroisoindoline, [$RuCl_3$·$3H_2O$], L	2-Ethoxyethanol, reflux, 24–48 h	[{2,9,16,23-(*t*Bu)$_4$Pc}RuL$_2$]	L = pyz, dabco, bpy, 2-Clpy, 3-Clpy, NH_3 Where L = pyz, DBU catalyst was used.	[76–78]
4-R-phthalonitrile, [$RuCl_3$·$3H_2O$], 3-Clpy	2-Ethoxyethanol, DBU, reflux, 24–72 h	[(2,9,16,23-R_4Pc)Ru(3-Clpy)$_2$]	R = *t*Bu, Me_3Si Where R = Me_3Si refluxing for extended periods gave tri- and di-substituted complexes	[78,80]
4-R-phthalonitrile, [$RuCl_3$·$3H_2O$]	Ethanol, DBU, 240 °C (autoclave), 2 h	[(2,9,16,23-R_4Pc)Ru]	R = Et, *t*Bu Subsequent report [79] suggests product is [{2,9,16,23-(*t*Bu)$_4$Pc}Ru(CO)]	[69]
4-*t*-Butylphthalonitrile, [$RuCl_3$·$3H_2O$]	Isoamyl alcohol, DBU, reflux, 12 h	[{2,9,16,23-(*t*Bu)$_4$Pc}Ru(CO)]	Lower yields obtained using *o*-dichlorobenzene as solvent	[79]
4-*t*-Butylphthalonitrile, [$RuCl_3$·$3H_2O$], iqnl	Quinoline, reflux, 4 h	[{2,9,16,23-(*t*Bu)$_4$Pc}Ru(iqnl)$_2$], [({2,9,16,23-(*t*Bu)$_4$Pc}Ru(iqnl))$_2$]	iqnl present as impurity in qnl. Dimer was minor product	[79]
4,5-Dipentyloxyphthalonitrile, [$RuCl_3$·$3H_2O$], L	2-Ethoxyethanol, DBU, reflux, 18–72 h	[{(2,3,9,10,16,17,23,24-$C_5H_{11}O)_8$Pc}Ru(L)$_2$]	L = 3-Clpy, 4-Mepy, methyl isonicotinate, isonicotinic acid. For the latter two ligands, *trans*-esterification was reported	[23,81]
3,6-Dipentyloxyphthalonitrile, [$RuCl_3$·$3H_2O$], 3-Clpy	2-Ethoxyethanol, DBU, reflux, 7 days	[{(1,4,8,11,15,18,22,25-$C_5H_{11}O)_8$Pc}Ru(3-Clpy)$_2$]		[39]
Dicyano-benzo-15-crown-5, Ru source	250 °C, 4 h	[{(15-crown-5)$_4$Pc}Ru(CO)(MeOH)]	Ru source = [$RuCl_3$·$3H_2O$], [$Ru_3(CO)_{12}$], [Ru(dmso)$_4Cl_2$], or [$Ru_2(OAc)_4Cl]_n$. MeOH possibly coordinated during chromatographic purification	[82–84]
Dicyano-benzo-15-crown-5, [$RuCl_3$·$3H_2O$], iqnl	Quinoline, reflux, 4 h	[(15-crown-5)$_4$PcRu(iqnl)$_2$]	iqnl present as impurity in qnl. Reaction failed using py as solvent	[84]
1,2-Dicyano-3,6-diheptyl-4,5-dimethylbenzene, [$RuCl_3$·$3H_2O$], 3-Clpy	2-Ethoxyethanol, DBU, reflux, 7 days	[{(1,4,8,11,15,18,22,25-$C_7H_{15})_8$(2,3,9,10,16,17,23,24-$CH_3)_8$Pc}Ru(3-Clpy)$_2$]		[85]
Tetrafluorophthalonitrile, [$Ru_3(CO)_{12}$]	1-Chloronaphthalene, reflux, 24 h	[(F_{16}Pc)Ru]		[86,87]
R_4-Phthalonitrile, [$Ru^{III}(NH_3)_5I]I_2$	240–250 °C	[R_{16}PcRu]	R = Cl, F Yield lowered using solvent or [$Ru^{III}(NH_3)_5Cl]Cl_2$	[88]
4,5-Dipentoxyphthalonitrile, 4,5-[(4-ethoxycarbonyl)phenoxy]phthalonitrile, [$RuCl_3$·$3H_2O$], 4Mepy	2-Ethoxyethanol, DBU, reflux, 48 h	[{2,3,9,10,16,17-(pentoxy)$_6$-23,24-{(4-pentoxycarbonyl)phenoxy}$_2$Pc}Ru(4-mepy)$_2$]	A *trans*-esterification reaction with the solvent was reported	[89]

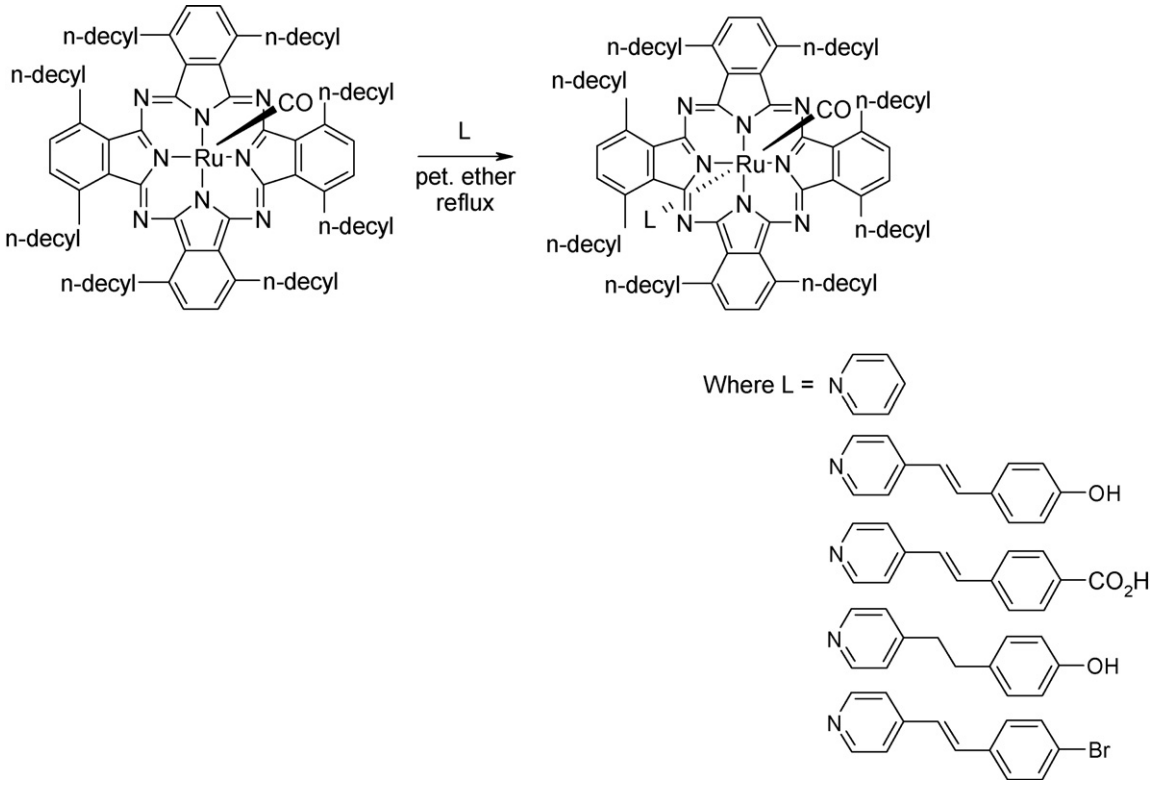

Scheme 7. Synthesis of some mono-carbonyl complexes [93].

$(Me_3Si)_4Pc\}Ru]$ with *t*-butyl-isocyanide afforded $[\{2,9,16,23\text{-}(Me_3Si)_4Pc\}Ru(tBuNC)_2]$.

2.2.4.3. Axial ligand exchange reactions. Treatment of $[\{1,4,8,11,15,18,22,25\text{-}(n\text{-decyl})_8Pc\}Ru(CO)]$ with various substituted pyridine ligands resulted in axially unsymmetrical products that retained the carbonyl ligand (Scheme 7) [93].

Rihter et al. found that irradiation of $[\{1,4,8,11,15,18,22,25\text{-}(OBu)_8Pc\}Ru(CO)(py)]$ in pyridine with a mercury lamp leads to decarbonylation, giving the corresponding bis-pyridine complex [91]. Decarbonylation was also achieved by heating the carbonyl complexes $[\{2,3,9,10,16,17,23,24\text{-}(C_5H_{11}O)_8Pc\}Ru(CO)]$ and $[\{2,3,9,10,16,17,23,24\text{-}(2\text{-Ethex}O)_8Pc\}Ru(CO)]$ with *t*-butyl isocyanide for extended periods (3 days), affording the corresponding bisaxial adducts [35,81].

Boiling the crown-substituted complex $[\{(15\text{-crown-}5)_4Pc\}Ru(CO)(CH_3OH)]$ in pyridine did not lead to decarbonylation, however with the addition of trimethylamine oxide, the reaction proceeded to completion in 3 h at room temperature [84,94]. Axial substitution with other ligands such as triethylamine [84], isoquinoline [84,94], pyrazine [94], and triethylenediamine [95] was also achieved although elevated temperatures were required. A drawback to the technique was the formation of $[\{(15\text{-crown-}5)_4Pc\}Ru\{(CH_3)_3N\}(L)]$ in significant (20%) yields.

The reaction of $[\{1,4,8,11,15,18,22,25\text{-}(n\text{-octyl})_8Pc\}\text{-}Ru(PhCN)_2]$ with two molar equivalents of either 4-methylpyridine or 4-dimethylaminopyridine readily gave the corresponding bisaxially substituted complexes [92,93]. Interestingly, using one equivalent of pyridine gave a 1:1 mixture of the bis-benzonitrile and bis-pyridine complexes.

Porphyrin/phthalocyanine supramolecular arrays were prepared by the coordination of pyridyl-substituted porphyrins to the vacant site of $[\{1,4,8,11,15,18,22,25\text{-}(n\text{-octyl})_8Pc\}Ru(CO)]$ [93]. From monopyridylporphyrin, a 1:1 Pn/Pc complex was obtained with the two macrocycles linked via a ruthenium-pyridine coordinative bond. From dipyridylporphyrin a 2:1 Pn/Pc array was produced with the dipyridylporphyrin forming bonds to two ruthenium phthalocyanine macrocycles. Similarly, tetrapyridylporphyrin resulted in a 4:1 Pn/Pc array.

2.2.5. Substituted dimeric and polymeric complexes

Dimeric complexes have been isolated as minor products from several reactions. The dimer $[\{(NaSO_3)_4PcRuOH\}_2O]\cdot 8H_2O$ was reported as a minor product of the reaction of potassium chlororuthenate with ammonium sulfophthalate [72]. In the reaction of 4-*t*-butyl-phthalonitrile with $[RuCl_3\cdot 3H_2O]$ in quinoline, the dimeric species $[(\{2,9,16,23\text{-}(tBu)_4Pc\}Ru(iqnl))_2]$ was identified with the Ru = Ru bond confirmed by Raman spectroscopy [79].

The first soluble phthalocyaninato-transition-metal oligomers were prepared by refluxing crude $[\{2,9,16,23\text{-}(tBu)_4\text{-}Pc\}Ru]$ in acetone with diisocyanobenzene and 2,3,5, 6-tetramethyl-1,4-diisocyanobenzene [75]. The chain lengths were estimated to be 10–14 units for $[\{2,9,16,23\text{-}(tBu)_4\text{-}Pc\}Ru(dib)]_n$ and 15–19 for $[\{2,9,16,23\text{-}(tBu)_4Pc\}Ru\text{-}(me_4dib)]_n$ by ^1H NMR spectroscopy. Refluxing the oligomers in chloroform for 24 h doubled the chain length.

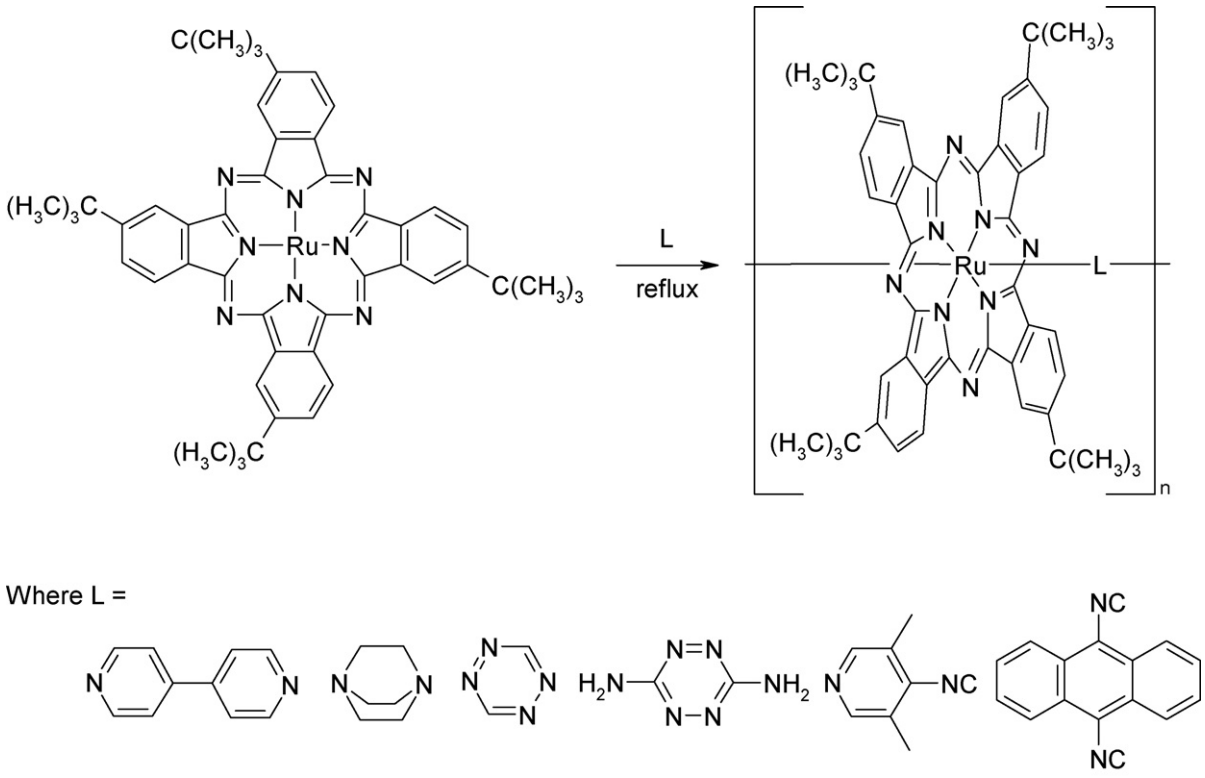

Scheme 8. Synthesis of axially bridged polymers from [{2,9,16,23-(tBu)$_4$Pc}Ru] [77].

Using pure [{2,9,16,23-(tBu)$_4$Pc}Ru], a variety of bridging ligands could be employed for polymer synthesis (Scheme 8). Refluxing [{2,9,16,23-(tBu)$_4$Pc}Ru] in acetone for 3 days with various ligands gave the corresponding oligomers in all but one case [77]. With pyrazine, low yields were obtained, however heating the monomer [{2,9,16,23-(tBu)$_4$Pc}Ru(pyz)$_2$] at 200 °C gave the desired oligomer. This procedure had been previously applied in the synthesis of [PcRu(pyz)]$_n$.

The tetra-*t*-butyl substituted oligomers [{2,9,16,23-(tBu)$_4$Pc}Ru(Medib)]$_n$, [{2,9,16,23-(tBu)$_4$Pc}Ru(Me$_2$dib)]$_n$, and [{2,9,16,23-(tBu)$_4$Pc}Ru(tBu$_2$dib)]$_n$ as well as the tetra-ethyl substituted oligomers [(2,9,16,23-Et$_4$Pc)Ru(dib)]$_n$, [(2,9,16,23-Et$_4$Pc)Ru(Medib)]$_n$, [(2,9,16,23-Et$_4$Pc)-Ru(Me$_2$dib)]$_n$, [(2,9,16,23-Et$_4$Pc)Ru(Me$_4$dib)]$_n$, and [(2,9,16,23-Et$_4$Pc)Ru(tBu$_2$dib)]$_n$ were also prepared using the above method [69]. The soluble oligomers had average chain lengths varying from 10 to 22 repeat units; the tetra-*t*-butyl oligomers having longer chain lengths, believed to be a result of their higher solubilities.

The octaalkoxy-substituted phthalocyanine complexes, [{2,3,9,10,16,17,23,24-(C$_5$H$_{11}$O)$_8$Pc}Ru(CO)] and [{2,3,9,10,16,17,23,24-(2-Et-hexO)$_8$Pc}Ru(CO)] were heated at 60 °C in acetone for 3 days with 1,4-diisocyano-2,3,5,6-tetramethylbenzene, to give the corresponding oligomers [81].

2.3. Synthesis of naphthalocyanine complexes

There are relatively few reports of ruthenium naphthalocyanine complexes. Those reported are 2,3-naphthalocyanine compounds where the naphthalene unit is incorporated into the macrocycle by the carbon atoms at the 2 and 3 positions of the naphthalene ring (see Fig. 5). Although 1,2-naphthalocyanine complexes have been reported for other metals, none has been reported incorporating a Ru metal centre.

Nalwa et al. [96] reported the first preparation of a ruthenium naphthalocyanine complex. The ring-substituted complex [{(t-Bu)$_4$-2,3-Nc}Ru] was prepared (see Fig. 5) using a modified synthetic method reported for [NcCu] and [NcV] complexes [97].

Hanack and Polley [98] prepared [2,3-NcRu(qnl)$_2$] from RuCl$_3$ and 2,3-naphthalonitrile in quinoline (Scheme 9). Thermolysis of the axial ligands gave impure [2,3-NcRu], believed to be a result of the greater thermal and oxidative sensitivity of the 2,3-Nc ring system compared to that of the Pc ring. Impure [2,3-NcRu] was also obtained by the reaction of 1-imino-1H-benz[*f*]-isoindol-3-amine and RuCl$_3$ in 2-ethoxyethanol with DBU as a catalyst (Scheme 9).

The "crude [2,3-NcRu]" from either method was purified by first coordinating N-donor ligands, followed by chromatography to yield [2,3-NcRuL$_2$] (L = pyridine, 3-chloropyridine, 2-ethylhexylamine, *t*-butylisonitrile). Thermal decomposition of [2,3-NcRuL$_2$] (where L = 3-chloropyridine or 2-ethylhexylamine) at 200 °C *in vacuo* yielded pure [(2,3-Nc)Ru]. Similarly prepared was pure [{(tBu)$_4$-2,3-Nc}Ru] by thermal decomposition of [{(tBu)$_4$-2,3-Nc}Ru(3-Clpy)$_2$] [78]. Interestingly, the *t*-butyl groups in [{(tBu)$_4$-2,3-Nc}Ru] did not impart high solubility to the product [78]. From pure [2,3-NcRu], the complexes [(2,3-Nc)Ru(BzNC)$_2$] and [2,3-NcRu(4,4′-

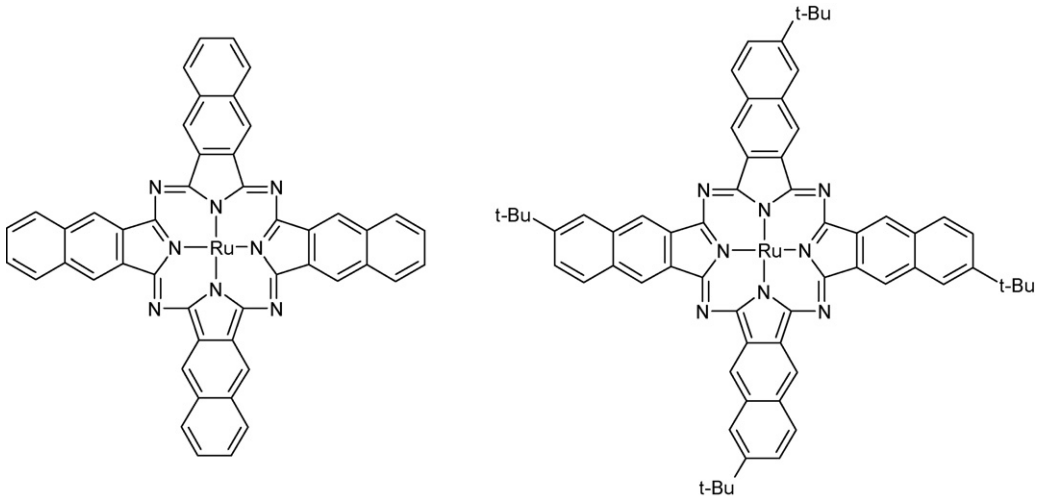

Fig. 5. [2,3-NcRu] (left), and [{(t-Bu)$_4$-2,3-Nc}Ru] (right, only one isomer shown).

bpy)$_2$] were prepared, and from [{(tBu)$_4$-2,3-Nc}Ru] was obtained [{(tBu)$_4$-2,3-Nc}Ru(pyz)$_2$] [77]. Although the related complexes [(PcRu)$_2$] and [({(tBu)$_4$Pc}Ru)$_2$] have been shown to be dimeric species (see Section 3.3), no reports describing the structure of the analogous Nc complexes have been reported to date.

Bossard et al. [99] extended their PcRu synthesis (see Section 2.1.1) to NcRu complexes. "Ruthenium blue", 2,3-naphthalonitrile and ammonia in refluxing 1-pentanol afforded [2,3-NcRu(NH$_3$)$_2$], which was reacted with benzonitrile to give [2,3-NcRu(PhCN)$_2$]. The labile benzonitrile ligands were readily replaced with amine, pyrazine, pyridine and phosphane ligands. Interestingly, the use of ligands bearing sulfonate or carboxylate groups imparts water solubility to the complexes.

NcRu polymers were prepared by heating [2,3-NcRu] with one molar equivalent of the bridging ligands 4,4′-bpy, dib, Me$_4$dib, dia, Me$_2$pyNC, tz, and dabco to give the corresponding axially bridged polymers [(2,3-Nc)RuL]$_n$. From [{(tBu)$_4$-2,3-Nc}Ru], the polymer [{(tBu)$_4$-2,3-Nc}Ru(bpy)]$_n$ was obtained under similar conditions [77]. The conduction properties of these polymers are discussed in Section 3.5.

3. Properties of ruthenium phthalocyanine and naphthalocyanine complexes

3.1. Spectroscopic properties

3.1.1. UV–vis absorption spectra

The typical six-coordinate ruthenium phthalocyanine complex has four main UV–vis absorption bands (see Fig. 6). The

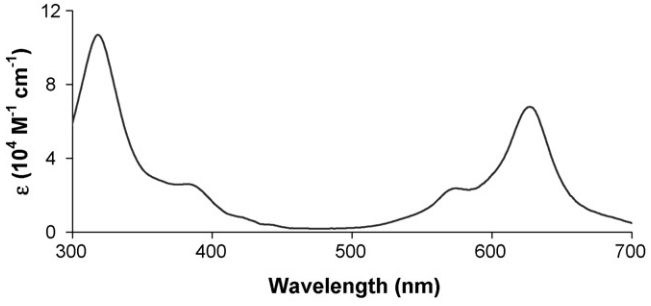

Fig. 6. UV–vis spectrum of [{2,9,16,23-(tBu)$_4$Pc}Ru(4-Mepy)$_2$] in dichloromethane.

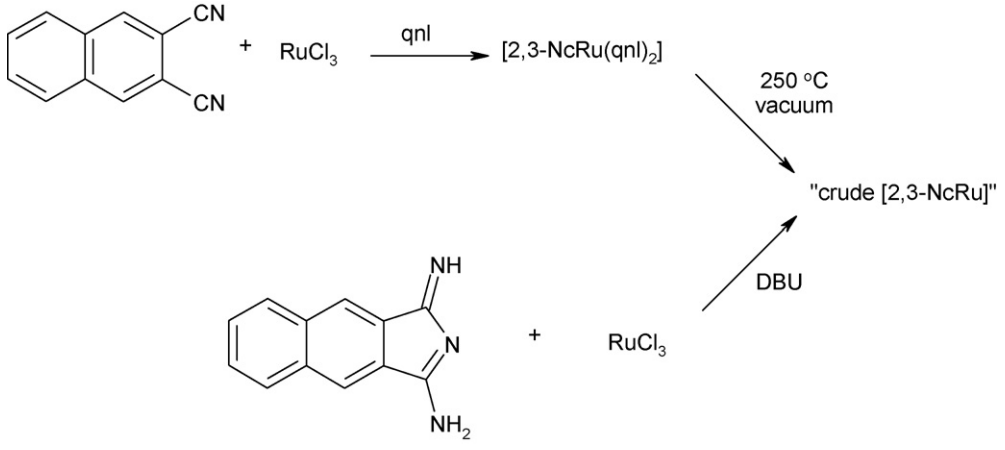

Scheme 9. Preparation of crude [2,3-NcRu] [98].

spectrum is dominated by the intense Q- and Soret bands, which are characteristic of phthalocyanine compounds in general [1]. An intense Q-band absorption is observed in the region 620–652 nm [20,22,32,44,85] and is assigned to a $\pi \rightarrow \pi^*$ transition within the macrocycle [1,24,74,84,87,94,100]. A single intense Q-band is observed in contrast to metal-free phthalocyanine, PcH_2, which has two bands of roughly equal intensity in this region due to deviation from D_{4h} symmetry caused by the two inner hydrogen atoms [101]. The Soret band (B-band) occurs in the region 300–325 nm [24,32,44,85], and is also attributed to a $\pi \rightarrow \pi^*$ transition of the macrocycle [24,84,94,100]. A relatively weak band, often seen as a shoulder to the Soret band, appears in the region 340–385 nm [20,44,84,94,102]. This weaker absorption has been attributed to a charge transfer (CT) transition [84,94,102] although the exact nature of the transition is unclear [103,104]. Accompanying the Q-band is a weak shoulder observed between 560 and 595 nm [1,20,24,44].

As well these four main bands, a band at ~270 nm has also been reported for the complexes [$PcRuL_2$] where L = pyz, Mepyz, Me_2pyz, Etpyz, *t*Bupyz, bpy, although the band was not assigned [1,32]. A weak band at 435–475 nm reported for the complexes [$PcRuL_2$] where L = the aromatic N-heterocycles qnx, Meqnx, qnz, ptz, qnl, pypyz, iqnl, npd and pyz, has been attributed to metal-to-ligand charge-transfer [44]. Aggregation of ruthenium phthalocyanine complexes in solution causes a weak absorption band to appear at ~430 nm [23].

Axially coordinated ligands such as N aromatic heterocycles, amines, and phosphanes appear not to have a significant effect on the Soret band energy although the Soret band experiences a pronounced hypsochromic shift of 500–1000 cm^{-1} when CO is axially coordinated [20,84,94].

The energy and intensity of the Q-band absorption are not uniform amongst complexes of the type [$PcRuL_2$]. Variations appear to be the result of differences in the nature of axial ligands. For various N-donor heterocyclic ligands, minor Q-band shifts are reported [44]. Coordination of a carbonyl ligand induces a bathochromic shift of 300–500 cm^{-1} and a significant increase in the molar absorptivity [20,84,94]. For example the Q-band of [$PcRu(py)_2$] appears at 622 nm with a molar absorptivity of 7.4×10^4 M^{-1} cm^{-1}, while [PcRu(CO)(py)] exhibits a Q-band with a maximum at 637 nm and a molar absorptivity of 1.7×10^5 M^{-1} cm^{-1} [20]. The Q-band of [PcRu(CO)(py)] splits into two bands at temperatures below 100 K in glassy matrices [105]. The splitting is believed to be a result of new steric and symmetrical properties imposed on the complex by solvation of the phthalocyanine and axial ligands, and the polar electronic influence of the solvents on the ligands.

Peripheral substitution of the macrocycle has only a weak influence on the position of the Q-band. Hanack et al. state that peripheral substitution with an electron-donating group causes a weak bathochromic shift of the Q-band [78]. Spectroscopic data from trimethylsilyl- [80], alkyl- [69,85,102], and alkoxy- [89,91] substituted ruthenium phthalocyanine complexes support this, all displaying bathochromic shifts. However, substitution with 15-crown-5 groups has no significant impact on the absorption spectrum [84,94]. The ring-perfluorinated complex [F_{16}PcRu] has a Q-band absorption reported at 616 nm [86,87], which is hypsochromically shifted compared to the [(PcRu)] dimer [100], although separate reports of the UV–vis spectra of [(F_{16}Pc)Ru] and [(Cl_{16}Pc)Ru] indicate a bathochromic shift compared to [$(PcRu)_2$] with Q band maxima at 632 and 644 nm respectively [88].

Dissolving [{(tBu)$_4$Pc}Ru$(py)_2$] and [(X_{16}Pc)Ru] (where X = Cl, F) in different organic solvents has little to no effect on the position of the Q-band [88,102] although a large bathochromic shift is observed using H_2SO_4 as solvent [25,27,72].

In the solid phase visible spectrum of the [$(PcRu)_2$] dimer, the Q-band absorbance is significantly red-shifted and broadened compared to solution measurements [100,106]. It is suggested that the cofacially assembled dimers form dome-like configurations in the solid state. The molecules form concave/convex pairs, and these structures have strong π–π intermolecular interactions forming molecular stacks in the solid state. In thin films of PcRu the Q-band is further red shifted [100].

For axially bridged polymers, the entire electronic spectrum is bathochromically shifted, with Q-band red-shifts of approximately 4–500 cm^{-1} reported depending on the bridging ligand [41,43,67,107]. Oxidation of the polymers with iodine causes a further ~400 cm^{-1} bathochromic shift of the Q band [67]. NIR absorption bands have been reported at ~870 and ~1065 nm for $[PcRu(tri)]_n$ and assigned to a charge-transfer from the metal d_{xy} orbital to a π^* triazine orbital [107]. The energy of this MLCT band is affected by metal-ligand π-backbonding; weaker π-backbonding causes the MLCT band to shift to higher energy and may become obscured by the strong Q-band.

The UV–vis spectra of ruthenium naphthalocyanine complexes involve mainly π–π^* transitions of the macrocycle [77,78]. For monomeric ruthenium naphthalocyanines, the Q-band is bathochromically shifted compared to ruthenium phthalocyanines, occurring mainly between 714 and 730 nm [77,78,98,99], although the spectrum of [2,3-NcRu] in H_2SO_4 contains a Q-band at 853 nm [98]. The Soret band occurs in the 311–325 nm region [78,98,99], similar to that of the ruthenium phthalocyanine analogs. The Q-band has a shoulder observed between 652 and 692 nm [78,98,99], and a shoulder to the Soret band at ~363 nm has also been reported [78,99]. Other unassigned absorption bands have been reported at 642 nm [78,98], and 420 nm [78,99]. Peripheral substitution with *t*-butyl groups causes a slight bathochromic shift of the Q-band [78], and polymerisation causes a significant bathochromic Q-band shift of about 500 cm^{-1} [98].

3.1.2. Infra-red spectra

Complexes of the type [$PcRuL_2$] have similar IR spectra to each other, with little influence from the axial ligand [44]. Bands at 519, 908, 1413 and 1489 cm^{-1} contain contributions mostly from the atoms in the Pc ring near to the metal [62], and so are sensitive to the central metal atom, although bands at 1064, 1288, 1443, and 1907 cm^{-1} have also been reported to be metal sensitive [8].

The spectrum of ruthenium phthalocyanine exhibits absorption bands at ~776 and 756 cm^{-1} of equal intensity while in the

spectra of [PcRuL$_2$] complexes the bands have unequal intensities [45]. [PcRuL$_2$] complexes also exhibit additional bands in their IR spectra arising from the axial ligands that are not present in the ruthenium phthalocyanine spectra [44].

For complexes with axial aromatic isocyanide ligands, for example [PcRu(dib)$_2$], υ(C≡N) of the coordinated ligand is observed at lower energy compared that of the free ligand [32,48,69,75,77,81,108]. In contrast, υ(C≡N) shifts to higher energy in coordinated aliphatic isocyanides [77,108]. In the case of aliphatic isocyanides, the sigma donation dominates the metal-ligand bond. Because the sigma-bonding electrons come from a weakly anti-bonding isocyanide MO [77], a rise in the υ(C≡N) stretching frequency is observed upon coordination. Aromatic isocyanides have enhanced π-accepting ability through electron delocalisation into antibonding molecular orbitals located on the aromatic ring [69,77]. This π-backbonding transfers electron density to a strongly antibonding isocyanide MO, thus lowering the bond order and υ(C≡N) stretching frequency upon coordination [77,108]. In the case of axially bridged polymers with aromatic isocyanide ligands, υ(C≡N) is shifted to even lower energy compared to the corresponding monomer [32,75,108]. Ruthenium phthalocyanine complexes with axial aromatic isocyanide ligands have υ(C≡N) at lower energy than the corresponding iron analogue due to the greater π backbonding ability of ruthenium [48,81]. Peripheral substitution of the macrocycle affects the position of υ(C≡N). Electron donors such as alkoxy groups increase the electron density at the ring, thus enhancing π-backbonding and lowering the υ(C≡N) energy [81]. The weakly electron donating *t*-butyl groups have no effect on the position of υ(C≡N) in di-isocyanide bridged polymers [75].

Coordinated alkynes exhibit a decrease in the frequency of υ(C≡C) compared to that of the free acetylene [45]. The acetylide anion's HOMO is weakly antibonding, therefore the increased electron density about the carbon in the anion destabilises the C≡C bonding MO, thus lowering the anion's υ(C≡C) frequency. Upon coordination, electron density is transferred to the ruthenium ion, stabilising the carbon–carbon triple bond and raising υ(C≡C) frequency to a level still below that of the free acetylene. In contrast, axial coordination of NH_3 shifts the N–H stretching frequencies to lower energy [107].

The IR spectra of complexes with axial carbonyl ligands have characteristic bands in the region 1934–1965 cm^{-1} assigned to υ(C≡O) [11,20,79,82,84].

The nitrido bridged complex, [(RuPc)$_2$N], has an IR spectrum that differs from ruthenium phthalocyanine only by the presence of a band at 1040 cm^{-1}, which is assigned to υ_{as}(Ru–N–Ru) [34]. In the heterobimetallic complex [(TTP)Fe–N–RuPc], υ_{as}(Fe–N–Ru) is at a similar energy of 1032 cm^{-1} [60]. Similarly [{RuPc}$_2$(μ-C)] has strong bands at 1034/1050 cm^{-1} assigned to υ_{as}(Ru–C–Ru) [62].

IR spectroscopy is useful for characterization of axially bridged ruthenium phthalocyanine polymers [32,77]. Polymerisation leads to changes in the symmetry of the bridging axial ligand, which can be observed in the IR spectrum. For example, there is greater local symmetry of the bridging pyrazine in [PcRu(pyz)]$_n$ compared to the monomer [PcRu(pyz)$_2$]. Thus some $C_{2\upsilon}$ vibrational modes for pyrazine in [PcRu(pyz)$_2$], e.g. centrosymetric ring-stretches, are not observed in the spectrum of the polymer. Additionally ligand vibrations allowed in both the terminal and bridging ligands are shifted, e.g. the out-of-plane C-H vibration of pyrazine shifts from 807 cm^{-1} in [PcRu(pyz)$_2$] to 815 cm^{-1} in [PcRu(pyz)]$_n$. IR spectroscopy has been used to determine the site of oxidation that follows doping with I_2 [67]. Iodine doping of the polymer [PcRu(ppd)]$_n$ produces a new absorption band at 1604 cm^{-1}, indicative of a quinoid structure of the oxidised *p*-phenylenediamine ligand, demonstrating ligand centred oxidation. After similar doping of [PcRu(apy)]$_n$ (where apy = 4-aminopyridine), some bands assigned to the Pc macrocycle disappear while the axial ligand absorption component remains relatively unchanged, suggesting Pc-centred oxidation.

IR spectroscopy has been used to distinguish different polymorphic forms of PcRu complexes. Comparison of [(PcRu)$_2$] as a bulk solid and as a thin film shows differences in the out-of-plane C–H bending region (800–700 cm^{-1}). This, and the absence of a peak at 866 cm^{-1} in the thin film specimen were attributed to different molecular assemblies [100]. A greater number of stacked dimers in the film is suggested as a possible cause of the spectral differences.

3.1.3. NMR spectra

The macrocyclic protons of ruthenium phthalocyanine complexes without peripheral substitution show an AA′BB′ pattern of multiplets at low field, typical of diamagnetic phthalocyanine compounds [13,14,19–21,24,32,40,44,48,50]. Resonances for β protons (see Fig. 7) have been reported as multiplets between δ 8.12 and 7.90. All α-proton (Fig. 7) resonances are reported as multiplets between δ 9.41 and 9.16. Inspection of the reported NMR data reveals that most axial ligands have an insignificant effect on the position of these resonances although axial carbonyl ligands generate a downfield shift [19,79,84].

Ruthenium 2,3-naphthalocyanine complexes without peripheral substitution (see Fig. 5) show three low field resonances

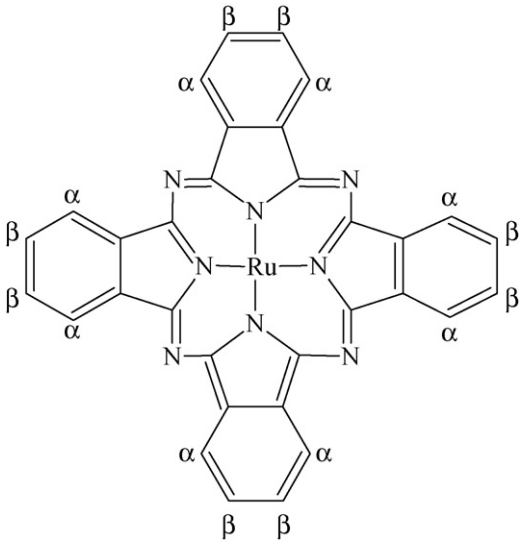

Fig. 7. Diagram showing designation of α and β protons in PcRu.

from the three non-equivalent macrocyclic positions at δ 9.83–9.60, 8.63–8.45 and 7.85–7.75 [77,98,99].

The ^{1}H and ^{13}C NMR spectra of ruthenium phthalocyanine and naphthalocyanine complexes lacking axial substitution show broad signals due to the paramagnetism of the square planar ruthenium(II) centre [78,81].

Tetra-substitution of the phthalocyanine ring generates three inequivalent ring proton positions that resonate at different frequencies. Often four constitutional isomers make up a tetra-substituted product and cause broadening of the macrocyclic proton signals. In [{2,9,16,23-$(Me_3Si)_4$Pc}Ru(3-Clpy)$_2$], multiplets at δ 9.35 and 9.17 are observed for the α-protons, and a doublet at δ 8.07 for the β-proton [80]. The macrocyclic protons of 2,9,16,23-tetra-*t*-butyl substituted ruthenium phthalocyanines exhibit a similar pattern but at slightly higher field [78,79]. For 2,9,16,23-tetra-ethyl substitution, macrocyclic proton resonances appear at higher field than those of tetra-*t*-butyl substituted complexes, and the two signals from the α-protons appear as one multiplet [69].

Tetra-substitution of ruthenium naphthalocyanines, as with phthalocyanines, reduces symmetry. Five resonances are observed for the macrocyclic protons. To date, NMR data for only two tetra-substituted ruthenium naphthalocyanines, [{(*t*Bu)$_4$-2,3-Nc}Ru(*t*BuNC)$_2$] and [{(*t*Bu)$_4$-2,3-Nc}Ru(3-Clpy)$_2$], have been reported. The macrocyclic resonances were observed at δ 9.70, 9.66, 8.43, 8.40 and 7.87 for [{(*t*Bu)$_4$-2,3-Nc}Ru(3-Clpy)$_2$] with similar values reported for [{(*t*Bu)$_4$-2,3-Nc}Ru(*t*BuNC)$_2$] [78].

For octaalkoxy peripherally substituted ruthenium phthalocyanines, where substitution occurs at the 2,3,9,10,16,17,23,24 positions, the α-proton resonance is shifted upfield to δ 8.54–8.71 [23,35,81]. Similarly, the α-proton resonance is observed at δ 8.50–8.58 with crown ether substitution in the 2,3,9,10,16,17,23,24 positions [84,94]. When octaalkoxy substitution occurs at the 1,4,8,11,15,18,22,25 positions, the β-protons appear as a single resonance shifted high field to δ 7.29–7.36 [39,91]. In 1,4,8,11,15,18,22,25 octaalkyl substituted complexes the β-proton resonance occurs at δ 7.76 [93].

Aggregation of [{(15-crown-5)$_4$Pc}Ru(CO)(CH_3OH)] causes an upfield shift of the macrocyclic protons by approximately 1 ppm [82]. The shift is explained by the ring current shielding effect of neighbouring molecules in aggregates.

With hexadecaalkyl-substitution, the aliphatic proton resonances are shifted downfield compared to those of the parent tetraalkyl phthalonitrile [85]. Similarly, upon cyclisation the resonances of the alkoxy group protons in octakis(pentyloxy) ruthenium phthalocyanines experience a slight downfield shift compared to the parent phthalonitrile [23,109]. For axially bridged polymers without peripheral substitution, the macrocycle AA′BB′ resonances shift by approximately 0.1 ppm upfield [32,69,108] compared to the corresponding monomers. For complexes with peripheral *t*-butyl or ethyl groups, the peripheral alkyl group resonances are also shifted upfield upon polymerisation [32,108].

Protons on axial ligands may be considerably shielded by the phthalocyanine diamagnetic ring current [13,14,32,44,45,78,84]. For example, the resonances of protons of the pyridine ligand in [PcRu(py)$_2$] occur at δ 2.43, 5.21 and 6.02, while the free ligand has the corresponding proton resonances at δ 8.60, 7.25 and 7.64, respectively [44]. The same shielding phenomenon is observed with ruthenium 2,3-naphthalocyanines, although the extent of shielding is not as large [78]. In [2,3-NcRu(py)$_2$] the pyridine resonances occur at δ 2.75, 5.30 and 6.10, which are still significantly shifted compared to the free ligand but are at lower field compared to the corresponding phthalocyanine complex [98]. Generally, ligand protons closer to the ruthenium centre experience greater shielding [45,78]. This is demonstrated in the series pyridine, pyrimidine, pyrazine, pyridazine, triazine and tetrazine, in which the extent of the upfield shift increases as the metal-ligand bond distance decreases [107].

NMR shift reagents have been used to simplify complex NMR spectra. When a compound has protons with similar chemical shifts, an NMR shift reagent can sometimes be added to the sample to separate overlapping peaks. The most commonly used NMR shift reagents are complexes of paramagnetic rare earth metals, e.g. tris(dipivalomethanato)europium. Alterations of chemical shift are brought about by coordination of the analyte to the complex. Due to their large ring currents, ruthenium phthalocyanine complexes have been examined as NMR shift reagents. [PcRu], [PcRu{$(CH_3)_2SO$}$_6$] and [PcRu{$(CD_3)_2SO$}$_6$] were successfully applied to a range of imidazoles, pyridines, hydrazines, primary, secondary and tertiary aliphatic amines, and primary and secondary aromatic amines [31]. Coordination via donor oxygen atoms did not occur, allowing some selectivity. Compared to iron phthalocyanines, the ruthenium analogues could be successfully applied to a larger variety of compounds.

3.2. Redox chemistry

3.2.1. Formal oxidation states of Ru in phthalocyanine complexes

Ruthenium coordination complexes exhibit a wide range of formal metal oxidation states [110]. The majority of reported PcRu and NcRu complexes have Ru(II) metal centres although a number of Ru(III) complexes have been reported [51,52,58]. The nitrido-bridged complex [(TTP)Fe–N–RuPc] also contains trivalent ruthenium [60] and [(PcRu)$_2$N] is reported to exist as a mixed valence Ru(III)–Ru(IV) species [34]. Ruthenium(IV) metal centres have been reported in [{($NaSO_3$)$_4$Pc}Ru(OH)$_2$] [72], the oligomeric complex HO–[PcRuO]$_n$–H [70], and in the μ-carbido complex [(PcRu)$_2$(μ-C)] and its pyridine adduct [61,62].

3.2.2. Electrochemistry

Table 3 shows electrochemical data for selected PcRu complexes. In the following discussion, electrochemical potentials are given relative to the ferrocenium/ferrocene couple (i.e. $Fc^+/Fc = 0$ V) to enable comparison of data from different sources (details of conversions from original data are given in the footnotes to Table 3). We start by examining [PcRuL$_2$] complexes where L are pyridine derivatives. Cyclic voltammetry experiments show that a reversible one-electron oxidation

Table 3
Electrochemical potentials, V vs. Fc^+/Fc for selected PcRu complexes

Compound	Redox process				Reference
	Pc^-, Pc^{2-}	Pc^0, Pc^-	Pc^{2-}, Pc^{3-}	Other	
[PcRu(py)$_2$]	0.31 (0.77)[a]	0.94 (1.40)[a]		−2.16 (−1.70)[b] $Pc^{3-,4-}$	[20]
	0.31 (0.77)[b]		−1.64 (−1.18)[b]		[111]
	0.19 (0.68)[c]	0.83 (1.32)[c]	−1.85 (−1.35)[c]		[54]
[PcRu(4-Mepy)$_2$]	0.28 (0.74)[a]	0.94 (1.40)[a]			[20]
[PcRu(4-*t*Bupy)$_2$]	0.24 (0.70)[a]	0.86 (1.32)[a]			[20]
[PcRu(3-Clpy)$_2$]	0.20 (0.67)[d]	0.90 (1.37)[d]	−1.77 (−1.30)[d]		[80]
[{$(Me_3Si)_4$Pc}Ru(3-Clpy)$_2$]	0.26 (0.73)[d]	0.98 (1.45)[d]	−1.67 (−1.20)[d]		[80]
[{$(Me_3Si)_3$Pc}Ru(3-Clpy)$_2$]	0.28 (0.75)[d]	1.00 (1.47)[d]	−1.67 (−1.20)[d]		[80]
[(*t*Bu_4Pc)Ru(3-Clpy)$_2$]	0.02 (0.49)[d]	0.75 (1.22)[d]			[80]
[PcRu(dmf)$_2$]	0.34 (0.80)[a]				[20]
[PcRu(dmso)$_2$]	0.43 (0.89)[a]				[20]
	0.32 (0.78)[e]		−1.53 (−1.07)[e]	−2.03 (−1.57)[e]	[111]
[PcRu(CH_3CN)$_2$]	0.26 (0.72)[a]				[20]
[PcRu(CN)$_2$]$^{2-}$	−0.16 (0.31)[f,g]	0.38 (0.85)[f,g]			[33]
	0.40 (0.89)[c]			−0.15 (0.34)[c], $Ru^{II,III}$	[54]
[PcRu(CO)(py)]	0.45 (0.91)[a]				[20]
	0.36 (0.85)[c]		−1.5 (−1.01)[c]		[54]
[PcRu(CO)(4-Mepy)]	0.42 (0.88)[a]				[20]
[PcRu(CO)(dmf)]	0.44 (0.90)[a]				[20]
[PcRu(CO)(Cl)]$^-$	0.13 (0.62)[c]		−1.68 (−1.19)[c]		[57]
[PcRu(CO)(Br)]$^-$	0.15 (0.64)[c]		−1.67 (−1.18)[c]		[57]
[PcRu(CO)(I)]$^-$	0.17 (0.66)[c]		−1.69 (−1.20)[c]		[57]
[PcRuCl_2]$^{2-}$	0.21 (0.70)[c]			−0.51 (−0.02)[c], $Ru^{II,III}$	[53]
[PcRuBr_2]$^{2-}$	0.21 (0.70)[c]			−0.44 (0.05)[c], $Ru^{II,III}$	[53]
[PcRu(NO_2)$_2$]$^{2-}$	0.34 (0.84)[h]			−0.19 (0.31)[h], $Ru^{II,III}$ 0.55 (1.05)[h], NO_2^-, NO_3^-	[56]
[PcRu(CN)(py)]$^-$	0.57 (1.06)[c]			−0.03 (0.46)[c], $Ru^{II,III}$	[54]
[PcRu(N_3)(py)]$^-$	∼0.56 (∼1.05)[c]			−0.15 (0.34)[c], $Ru^{II,III}$	[54]
[PcRu(NCO)(py)]$^-$	∼0.56 (∼1.05)[c]			−0.09 (0.40)[c], $Ru^{II,III}$	[54]
[PcRu(NO_2)(py)]$^-$	∼0.56 (∼1.05)[c]			−0.02 (0.47)[c], $Ru^{II,III}$	[54]
[(F_{16}Pc)Ru]	0.68[i]		−1.35[i]	−1.78[i], $Pc^{3-,4-}$	[88]
[(Cl_{16}Pc)Ru]	0.45[i]		−1.41[i]	−1.93[i], $Pc^{3-,4-}$	[88]

Original data in parentheses.
[a] In 0.05 M [*t*Bu_4N][PF_6] in CH_2Cl_2. Original data reported vs. SCE; converted using $E_{Fc+/Fc} = E_{sce} - 0.46$ V [112].
[b] In 0.1 M [*t*Bu_4N][PF_6] in CH_2Cl_2 containing 2% pyridine. Data vs. SCE converted using $E_{Fc+/Fc} = E_{sce} - 0.46$ V [112].
[c] In 0.1 M [*t*Bu_4N][ClO_4] in CH_2Cl_2. Original data reported vs. Ag/AgCl; converted using $E_{Fc+/Fc} = E_{Ag/AgCl} - 0.49$ V. This value for $E_{Fc+/Fc}$ was reported with the original data.
[d] In [*t*Bu_4N][PF_6] in CH_2Cl_2 (conc. not reported). Original data reported vs. SCE; converted using $E_{Fc+/Fc} = E_{sce} - 0.46$ V [112].
[e] In CH_2Cl_2-dmso. Data vs. SCE converted using $E_{Fc+/Fe} = E_{sce} - 0.46$ V [112].
[f] In 0.05 M [*t*Bu_4N][ClO_4] in CH_2Cl_2. Original data reported vs. SCE; converted using $E_{Fc+/Fc} = E_{sce} - 0.47$ V. This value for $E_{Fc+/Fc}$ was reported with the original data.
[g] This assignment questioned in a later report [54].
[h] In 0.1 M [*t*Bu_4N][ClO_4] in CH_2Cl_2. Original data reported vs. SCE; converted using $E_{Fc+/Fc} = E_{sce} - 0.50$ V. This value for $E_{Fc+/Fc}$ was reported with the original data.
[i] In 0.1 M [*t*Bu_4N][ClO_4] in benzonitrile. Data reported vs. Fc^+/Fc.

process occurs in the region 0.2–0.3 V, and a second oxidation occurs in the region 0.8–0.9 V. Spectroelectrochemical studies indicate that these processes both involve oxidation of the phthalocyanine macrocycle [20,80] to give $[Pc^-Ru^{II}L_2]^+$ and $[Pc^0Ru^{II}L_2]^{2+}$species, respectively. One-electron reduction processes have been observed in complexes of this type at ∼ −1.8 V and are assigned to reduction of the macrocycle [80]. The difference of ∼2 V between the first reduction and oxidation processes

appears typical for this type of complex. Substitution of the periphery of the macrocycle has a significant effect on the potential of the first and second oxidation processes as shown in the series where L = 3-Clpy and the periphery has H, *t*-Bu or Me_3Si groups [80].

Complexes with dmf, dmso and acetonitrile axial ligands show similar behaviour to the complexes with axial pyridine ligands upon one-electron oxidation but a second oxidation process has not been reported [20]. The monomeric complexes [$(X_{16}Pc)Ru$] where X = F, Cl, also exhibit similar redox behaviour although the reduction and oxidation potentials are shifted to more positive values [88].

Complexes of the type [PcRu(CO)L] where L = py, 4-Mepy, or dmf show only one oxidation process at more positive potentials than the corresponding [$PcRuL_2$] complexes [20], which may be expected due to greater π-backbonding of ligated CO compared to pyridine ligands [113].

The first oxidation of $[PcRu(CN)_2]^{2-}$ at −0.16 V is quasireversible and is significantly more negative compared to the abovementioned complexes. This process was originally proposed to be a phthalocyanine ligand oxidation process [33], in line with previous studies of complexes with N-donor/π-acceptor axial ligands. Upon reduction of the oxidized species, an intermediate formed, which required the addition of CN^- to regenerate the starting complex. It was concluded that the oxidised species lost one axial ligand, with electrolyte occupying the vacant coordination position. Later, Homborg et al. [54] compared the electrochemistry of this complex with that of $[PcRu(CN)(py)]^-$, [$PcRu(py)_2$], and [PcRu(py)(CO)] and concluded that the first oxidation was a Ru(II)/Ru(III) metal-centred process. A second oxidation at 0.40 V was ascribed to the oxidation of the macrocycle, which is in agreement with potentials for this process in other PcRu complexes. It was reasoned that the absence of π-accepting ligands shifts the metal oxidation potential to a more negative value than that of the macrocycle. Substitution of one CN^- ligand for a pyridine ligand does not reverse the trend; $[PcRu(CN)(py)]^-$ has an oxidation process at 0.03 V, which is more positive than the dicyano complex but is still ascribed to a metal-centred oxidation. A second oxidation at 0.57 V is ascribed to the first macrocycle oxidation process. Interestingly, while the first oxidation for the complexes $[PcRuX_2]^{2-}$, where X = Cl, Br, is metal-centred, the first oxidation for $[PcRuX(CO)]^-$ is ring-based. Again, this appears to be a manifestation of the greater π-backbonding capability of CO compared to pyridine ligands.

The complex $[PcRu(NO_2)_2]^{2-}$ undergoes three one electron quasi-reversible oxidation processes at 0.31, 0.84 and 1.05 V [56]. The first process was reported to be metal-centred oxidation and the second process macrocycle-based oxidation. The third process was reported to be oxidation of the nitrite ligand although processes at this potential were observed in $[PcRuX(py)]^-$, where L = CN^-, N_3^-, NCO^-, NCS^-, suggesting that the oxidation is axial ligand independent [54].

Dimeric complexes display somewhat different redox behaviour to monomeric complexes. [$(PcRu)_2$] in tetrahydrofuran solution forms the solvated complex [$\{PcRu(thf)\}_2$]. It undergoes two reversible oxidations at 0.02 and 0.52 V, and three reduction processes at −0.59, −1.01, and −1.84 V (versus Fc^+/Fc) of which the last is irreversible [111]. The two oxidation processes were reported to involve metal-centred oxidation although the possibility of ring-based oxidation was not excluded. The first two reduction processes were reported to involve addition of electrons into metal $d(\pi^*)$ orbitals giving Ru^I–Ru^I species. The third reduction step was reported to be two-electron reduction of the phthalocyanine macrocycles. When [$\{PcRu(thf)\}_2$] was deposited onto graphite electrodes, the four reversible redox processes discussed above were observed at approximately the same potentials using thf as solvent. In aqueous acidic environment, only the first two reduction steps were observed, while in alkaline solution these two steps as well as the first oxidation step are observed.

The μ-carbido complex, [$\{PcRu(py)\}_2(\mu\text{-}C)$], undergoes four quasi-reversible one-electron-transfer processes [62]. Two reduction processes, at −1.62 and −1.88 V (versus Fc^+/Fc), involve reduction of the phthalocyanine macrocycles to form $[\{Pc^{3-}Ru(py)\}_2(\mu\text{-}C)]^{2-}$. Oxidation processes at 0.05 and 0.50 V are also ligand directed, giving the stable complex $[\{Pc^-Ru(py)\}_2(\mu\text{-}C)]^{2+}$.

The ruthenium naphthalocyanine, [(2,3-Nc)$Ru(py)_2$], has an oxidation process at ∼0.02 V and two reductions at −1.70 and −2.16 V (in pyridine versus Fc^+/Fc, original data: 0.48 V, −1.24, −1.70 V versus SCE) [98]. The oxidation and the first reduction are assigned to naphthalocyanine macrocycle-based processes. The more negative oxidation potential and reasonably invariant first reduction potential, compared to the analogous PcRu complex, is consistent with the trend for other metallonaphthalocyanine complexes [114].

3.2.3. Chemical redox properties

Chemical oxidation of [$PcRuL_2$] where L = pyridine derivatives, dmf, and dmso, to the cation $[Pc^{1-}RuL_2]^+$ was achieved using bromine with no ligand exchange observed. The radical cation was readily reduced back to its original form with dithionite [20,33]. Oxidation of $[PcRu(CN)_2]^{2-}$ with ferric chloride initially involves axial ligand exchange to give $[PcRu(CN)(Cl)]^{2-}$, which subsequently oxidised to the π-cation radical [33]. We reiterate here that Homborg et al. suggested that the first oxidation process of $[PcRu(CN)_2]^{2-}$ is metal-centred (from electrochemical experiments) so it is possible that the chemical oxidation process described by Nyokong [33] may also involve oxidation of the metal. [$PcRu(dmf)_2$] in dmf reacts with O_2 and irreversible oxidation of the Pc ligand is indicated [20]. Oxidation was not observed upon addition of I_2, Ce^{4+}, $[Fe(phen)_3]^{3+}$ or O_2 in dichloromethane [20]. Oxidation of $[Pc^{2-}Ru(CO)(X)]^-$, where X = Cl or Br, with the corresponding halogen or dibenzoylperoxide gave $[Pc^-Ru(CO)(X)]$ [57] and oxidation of $[Pc^{2-}RuX_2]^-$ (X = Cl or Br) with molecular halogen, X, gave $[Pc^-RuX_2]$ [58]. Similarly, reacting $[Pc^{2-}Ru(OH)_2]^-$ with iodine forms $[Pc^-RuI_2]$ [58]. $[Pc^{2-}Ru^{III}(OH)_2]^-$ was reduced by CO to give $[Pc^{2-}Ru^{II}(H_2O)(CO)]$ [55] and reaction of $H[Pc^{2-}Ru^{III}Cl_2]$ with $(n\text{-}Bu_4N)NO_2$ also reduces the metal centre to form $[Pc^{2-}Ru^{II}(NO_2)_2]^{2-}$ [56].

The dimer [(TTP)Fe–N–RuPc] formed a stable oxidised species when treated with I_2 [60]. Although the IR spectrum did not exhibit characteristic π-cation radical bands, the oxidation was reported to involve one of the macrocycles rather than a metal centre. Reduction of this species with $NaBH_4$ returned the dimer to its original state.

PcRu polymers may potentially be oxidized at the macrocycle, the ruthenium metal centre or the bridging ligand. Hanack et al. synthesised three PcRu polymers, two with bridging ligands with relatively low oxidation potentials (*p*-phenylenediamine and 2,7-diaminofluorene) and one with a higher oxidation potential, 4-aminopyridine [67]. Iodine oxidised the bridging ligands in the $[PcRu(ppd)]_n$ and $[PcRu(daf)]_n$ polymers (as evidenced by IR spectroscopy) while oxidation of the macrocycle occurred in $[PcRu(apy)]_n$.

3.2.4. Photo-redox properties

Excitation of ruthenium phthalocyanine complexes at Q-band wavelengths can generate reactive low-lying $\pi\pi^*$ triplet excited states. Electron transfer to electron acceptors may occur to form π-cation radical species [33,115]. Q-band excitation of $[PcRu(L)_2]$ (where L = py, dmf) followed by quenching with nitroaromatics or paraquat derivatives gave a ruthenium(II) phthalocyanine radical, $[Pc^{-}Ru^{II}(L)_2]^{+}$ [116,117]. Q-band irradiation of $[PcRu(dmso)_2]$, [PcRu(py)CO] and [PcRu(dmf)CO] also produces the $^3\pi\pi^*$ excited state but instead of electron transfer to the nitroaromatic or paraquat compounds, exciplexes were formed which simply dissociate to regenerate the original phthalocyanine complex [117]. The use of other quenching agents induced an electron transfer process in CO-, dmf- and dmso-containing ruthenium phthalocyanine complexes [115]. For example, Q-band irradiation of [PcRu(4-Mepy)(CO)] in the presence of CBr_4 at room temperature gave the π-cation radical $[Pc^{-}Ru^{II}(4\text{-Mepy})(CO)]^{\bullet+}$ in an irreversible reaction. The π-cation radical $[Pc^{-}Ru^{II}(py)_2]^{\bullet+}$ was formed reversibly at 79 K using 2,3-dichloro-5,6-dicyanobenzoquinone as an electron acceptor. Recovery of the parent phthalocyanine was achieved by warming the solution to 95 K.

Ultraviolet irradiation of $[PcRu(py)_2]$ led to the transient formation of reduced radical species [118]. The fate of the radical is solvent dependant. In dichloromethane, photodecomposition is observed, while in CO-saturated benzene or acetonitrile solutions photosubstitution of an axial pyridine ligand occurs.

3.3. Structural properties

3.3.1. Single-crystal X-ray diffraction studies

Although many crystal structures of phthalocyanine compounds have been reported [119], there are few reports of single-crystal X-ray diffraction studies of ruthenium phthalocyanine complexes. Selected data for the five complexes reported to date are shown in Table 4. All have a six-coordinate ruthenium atom at the centre of the macrocycle with axial ligands in the expected *trans* configuration. We note that in all cases, the $Ru–N_{iso}$ distance (where N_{iso} is the coordinated N atom of the Pc ring) is shorter that $Ru–N_{axial}$ (N_{axial} is the coordinated N atom of the axial ligand).

The crystal structure of $(^nBu_4N)_2[RuPc(NO_2)_2]$ consists of layers of $[RuPc(NO_2)_2]^{2-}$ anions separated by layers of $^nBu_4N^+$ cations [56]. There is no Pc–Pc overlap within the complex-containing layer and the macrocycle is slightly distorted from planarity. The *trans* nitro groups are staggered with respect to each other and have the shortest $Ru–N_{axial}$ bond length of any of the reported PcRu complexes.

In the crystal structure of $(^nBu_4N)[RuPc(py)(CN)]$, the unit cell contains four crystallographically independent complex anions [54]. The Ru atoms are drawn slightly from the N_4 plane of the coordinated macrocyclic N atoms towards the cyanide ligands by ~0.020 Å. The macrocycle itself is slightly distorted in a dome-like fashion towards the cyanide ligand. The *trans* ligands are slightly nonlinear with respect to the metal centre with the average angle $\angle(N_{axial}–Ru–C_{axial}) \sim 175^\circ$.

In the structure of the peripherally substituted $[\{(15\text{-crown-}5)_4Pc\}Ru(TED)_2]$ where TED = triethylenediamine, the Ru atom is exactly in the macrocyclic N_4 plane [95]. The structure contains chloroform molecules of solvation located between crown ether moieties and is unstable at room temperature. The seven chloroform molecules of solvation (per complex molecule) lie between crown ether rings of neighbouring molecules, which allows a "brickwork"-like stacking arrangement [120]. A $Ru–N_{TED}$ distance of 2.244 Å was found, which is slightly longer than the $Ru–N_{axial}$ distances found for other

Table 4
Selected X-ray diffraction data for some ruthenium phthalocyanine complexes

	$(^nBu_4N)_2[RuPc(NO_2)_2]$	$(^nBu_4N)[RuPc(py)(CN)]$	$[PcRu(4\text{-Mepy})_2]$	$[\{(15\text{-crown-}5)_4Pc\}Ru(TED)_2]$	$[PcRu(py)]_2(\mu\text{-C})]$
Crystal system	Monoclinic	Orthorhombic	Orthorhombic	Triclinic	Orthorhombic
Space group	$P121/n1$ (no. 14)	$Pca2_1$ (no. 29)	$Pcab$ (no. 61)	$P\bar{1}$ (no. 2)	$P2_12_12_1$ (no. 19)
a (Å)	15.114(4)	28.319(5)	10.2409(8)	12.9717(11)	13.002(3)
b (Å)	22.34(3)	29.850(3)	17.6893(14)	15.9309(14)	22.635(6)
c (Å)	18.206(11)	24.566(7)	24.465(2)	18.1636(16)	23.901(6)
α (°)				91.749(2)	
β (°)	90.88			107.037(2)	
γ (°)				112.993(2)	
Z	4	16	4	1	4
$Ru–N_{iso}$ (Å)	1.978(6)	1.947(2)–1.992(2)	1.991(3), 1.985(4)	1.983(3)–1.994(3)	2.010(8)
$Ru–N_{ax}$ (Å)	2.068(5)	2.141(14)–2.226(13)	2.101(4)	2.244(3)	2.328
$Ru–C_{ax}$ (Å)		1.97(2)–2.02(2)			1.77(1)

PcRu monomeric complexes. The axial ligands are linear with $\angle(N_{TED}–Ru–N_{TED}) = 180°$.

The complex [PcRu(4-Mepy)$_2$] crystallizes with a centrosymmetric complex molecule and two chloroform molecules of solvation [47]. The Ru–N_{iso} bond lengths are similar to those of the other PcRu examples and the overall macrocycle geometry was reported to be similar to that of the bis-nitro complex (discussed above). The two axial 2-methylpyridine ligands are coplanar and are oriented at 45° relative to Ru–N_{iso} bond vectors (i.e., the plane of the 2-methylpyridine ligands intersects the macrocyclic plane through the non-coordinating macrocyclic N atoms). The longer Ru–N_{axial} bond lengths were related to ease of replacement.

The μ-carbido bridged dimer [{PcRu(py)}$_2$(μ-C)] has a convex staggered conformation of the macrocycles with the Ru atoms essentially in the centre of the macrocyclic plane [61]. The almost linear Ru–C–Ru core has bond lengths of 1.77 Å, and the Ru–N_{py} bond is 2.010 Å. This structure is isostructural with the analogous iron complex [{PcFe(py)}$_2$(μ-C)] [61].

3.3.2. Structural properties of powders and films

Large-angle X-ray scattering (LAXS) was used to examine the structure of [(PcRu)$_2$] in the powder form [37,121]. The experimental data indicated that the material consists of dimers with an average of six molecular units stacked in one-dimensional arrays. A short intradimer Ru–Ru distance of 2.40 Å was reported with interdimer Ru–Ru distances of 4.30–4.40 Å. Structural data are shown in Fig. 8.

Each ruthenium atom was shown to be 0.41 Å out of the inner N_4 macrocyclic plane with the phthalocyanine rings adopting a slightly domed conformation. Extended X-ray absorption fine structure (EXAFS) experiments by Rossi et al. [122,123] were in agreement with the LAXS studies. EXAFS experiments by the research groups of Bertagnolli and Hanack [46] yielded an intradimer Ru–Ru distance of 2.41 Å, in agreement with the results described above, but a Ru–Ru interdimer distance of 3.52 Å was reported. This shorter interdimer distance was later questioned [121] as it implies a distance of 2.54 Å between neighbouring macrocycles, which is shorter than the intra-dimer Pc–Pc distance and too short for a contact caused

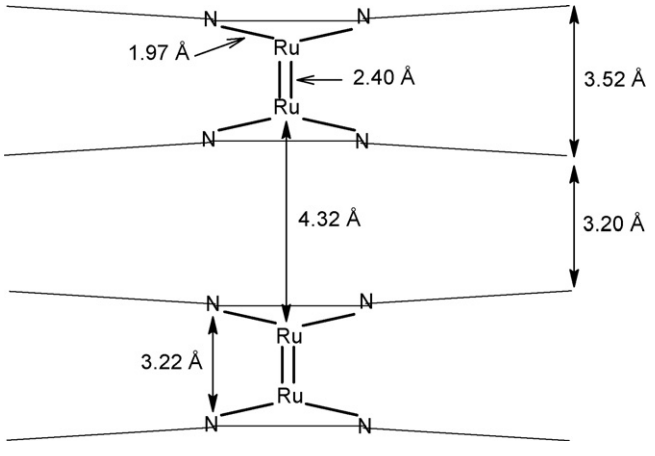

Fig. 8. Structural data for [(PcRu)$_2$] from Capobianchi et al. [37].

only by van der Waals interactions. Thin films prepared by evaporation were shown by EXAFS to consist of [(PcRu)$_2$] dimers, with similar bond distances to the powder samples although the distance between Ru and the four inner nitrogens of the neighbouring intradimer macrocycle increased slightly and the interdimer Ru–Ru distance decreased marginally [100]. Energy dispersive X-ray diffraction (EDXD) experiments of thin films indicated a greater ordering of dimers compared to bulk samples [124].

A room-temperature magnetic moment of 2.54 μ_B was measured for [(PcRu)$_2$] [37], which is indicative of two unpaired electrons. Because solid [(PcRu)$_2$] is EPR silent, this paramagnetism was not assigned to ligand-centred π-radical species [37]. Comparison of the data with that of other d^{12} ruthenium dimers [125] suggests a molecular orbital configuration of $\sigma^2\pi^4\delta^{nb4}\pi^{*2}$ (for a staggered conformation) and the presence of a Ru–Ru double bond, in agreement with the structural data from X-ray experiments.

[({2,9,16,23-(*t*Bu)$_4$Pc}Ru)$_2$] was shown by EXAFS to have a dimeric structure similar to that of [(PcRu)$_2$] [39] with the Ru atom approximately 0.4 Å out of the macrocyclic plane. An intradimer Ru–Ru distance of 2.42 Å was reported, which is similar to that reported for [(PcRu)$_2$], indicating that the *t*-butyl groups do not sterically hinder dimer formation.

Magnetic data for [({2,9,16,23-(*t*Bu)$_4$Pc}Ru)$_2$] are also supportive of the dimeric structure. It was argued that the spin-only value of 1.73 μ_B per monomer unit, i.e. [{2,9,16,23-(*t*Bu)$_4$Pc}Ru], indicates one unpaired electron but a square planar d^6 complex is expected to have two unpaired electrons. Again, a molecular orbital configuration of $\sigma^2\pi^4\delta^{nb4}\pi^{*2}$ is presented, which accounts for the presence of a Ru–Ru double bond and two unpaired electrons [78].

The structures of complexes bearing axial ligands have also been investigated by EXAFS. [PcRu(3-Clpy)$_2$] was shown to have an octahedral arrangement [39] with a Ru–$N_{(3\text{-}Clpy)}$ distance of 2.53 Å, which is larger than those reported for single-crystal structures determined by X-ray diffraction. An out-of-plane Ru displacement was considered unlikely, and the macrocycle was assumed to be nonplanar. [PcRu(3-Fpy)$_2$], [{2,9,16,23-(*t*Bu)$_4$Pc}Ru(3-Clpy)$_2$] and [{1,4,8,11,15,22,25-($C_5H_{11}O$)$_8$Pc}Ru(3-Clpy)$_2$] appear to have similar structures [39]. EXAFS measurements of [PcRu(py)$_2$] suggested that the ruthenium atom was located in the centre of the inner N_4 phthalocyanine plane, despite long Ru–N_4 bond lengths of 2 Å. The two axial pyridine ligands were found to be *trans*-coordinated with an Ru–N_{py} bond length of 2.53 Å [122,123]. This arrangement is similar to analogous iron phthalocyanine complexes. EXAFS data for [PcRu(*n*-butylamine)$_2$] surprisingly fitted best to a structure where the two amine ligands are coordinated on the same side of the macrocycle via long bonds of 2.52 Å, and on the opposite side to the out-of-plane Ru atom [46]. Neighbouring Ru atoms were separated by 4.13 Å with the macrocycles separated by at least 4.69 Å.

EXAFS was used to study the axially bridged ruthenium polymers [PcRu(tz)]$_n$, [PcRu(pyz)]$_n$, and [PcRu(dib)]$_n$ [65]. From the data, the Ru–$N_{(tz)}$ and Ru–$N_{(pyz)}$ distance was 2.22 Å, and Ru–$C_{(dib)}$ was 2.33 Å. All three oligomers studied had a six-

coordinate octahedral arrangement around the Ru atom with bridging axial ligands on both sides of the macrocycle. Small differences in the environments of the Ru atoms were observed. The macrocycle in $[PcRu(tz)]_n$ was determined to be nonplanar, while the Ru atom in $[PcRu(pyz)]_n$ was located slightly out of the N_4 plane.

LAXS studies of HO–$[PcRuO]_n$–H reveal that it adopts a columnarly stacked arrangement with a linear O–Ru–O–Ru– backbone (Ru–O is 1.845 Å) [70]. The ruthenium lies in the centre of the planar phthalocyanine ring. Adjacent macrocycles are 3.69 Å apart and have a relative rotation of 35°, with alternate macrocycles eclipsing each other. A subsequent EXAFS study supported the LAXS measurements [122,123]. The Ru–O bond distance was determined to be 1.807 Å with the macrocycles 3.719 Å apart.

3.4. Kinetic studies

Axial ligand substitution kinetics have been studied for a variety of PcRu complexes.

$$[PcRuL_2] + X \rightarrow [PcRuLX] + L \quad (1)$$

Kinetic data for reactions of the type shown in Eq. (1) where $L = P(OBu)_3$ and X = Meim, py, or PBu_3 are consistent with a dissociative (D) mechanism [13]. That is,

$$[PcRuL_2] \underset{k_2}{\overset{k_1}{\rightleftharpoons}} [PcRuL] + L$$

$$[PcRuL] + X \underset{k_4}{\overset{k_3}{\rightleftharpoons}} [PcRuLX]$$

Interestingly, in the case where $L = P(OBu)_3$ and X = Meim, k_1 and k_4 were found to be the same within experimental error. That is, forward and reverse rates are identical. In the case where X = py, k_4 was found to be larger than k_1. The ratios k_3/k_2 were found to be close to unity showing that the five coordinate intermediate does not discriminate between incoming ligands and is quite reactive. Comparison with kinetic data for the corresponding PcFe complexes showed that the PcRu complexes are more inert to substitution. In substitution reactions of [PcRu(Meim)(L)], 1-methylimidazole greatly deactivates the *trans* ligand, L compared to $[PcRu\{P(OBu)_3\}(L)]$ complexes. Leaving group effects in this type complex are, in terms of lability, py > Meim > $P(OBu)_3$.

Axial substitution reactions of benzylisocyanide (BzNC) and CO complexes also proceed by a dissociative (D) mechanism [14]. Again, coordinated Meim greatly deactivates the *trans* ligand. The π-acceptor ligands BzNC and CO, in contrast, have a strong *trans* labilizing effect. The relative lability of complexes with one BzNC ligand and one Meim or 4-*t*-butylpyridine ligand is RuPc < RuPorphyrin ≪ FePc < FePorphyrin. The PcRu/PcFe comparison is in agreement with earlier data [13].

Kinetic studies of the reaction of cyanide with [PcRu(CO)(DMF)] and $[PcRu(dmso)_2]$ [33] showed that with a large excess of cyanide, $[PcRu(CN)_2]$ forms under pseudo-first-order kinetics, with substitution proceeding in a stepwise fashion. The second substitution process was identified as the rate determining step with specific rate constants of 5.2×10^{-2} and $7.2 \times 10^{-2}\ M^{-1}\ s^{-1}$ for the dmf and dmso complexes, respectively.

Prasad and Ferraudi [118] investigated the photo-induced ligand substitution reaction of $[PcRu(py)_2]$. Irradiation with wavelengths of ~640 nm resulted in a radical transient species. This Ru(II) ligand radical mediates the substitution of one pyridine ligand but also facilitates photodecomposition of the complex. Irradiating $[PcRu(py)_2]$ in CO-saturated benzene or dichloromethane gave [PcRu(py)(CO)] on a millisecond timescale but irradiation in neat dichloromethane leads to decomposition by opening of the macrocycle.

3.5. Conduction properties of polymers

This section discusses electrical conductivity measurements of polymeric complexes formed by the axial coordination of ligands capable of bridging two ruthenium metal centres (see, for example, Fig. 2). The synthesis of this class of complex is discussed in Sections 2.1.4 and 2.2.5. Table 5 shows conductivity data for powder samples pressed into pellets and measured using either two- or four-point probe methods, and is predominately from the research of Hanack et al.

The first trend evident from the data is the large increase in conductivity that occurs upon polymerization. Conductivities of monomer complexes fall in the range 10^{-9} to $10^{-11}\ S\ cm^{-1}$. The increase in conductivity upon polymerization ranges from 3 to 9 orders of magnitude, indicating that as well as polymerisation, the nature of the bridging ligand has a significant effect. For example, the polymer $[PcRu(tz)]_n$ has a relatively high conductivity of $1 \times 10^{-2}\ S\ cm^{-1}$ while the polymer with dabco bridging ligands has a very low conductivity of $1 \times 10^{-9}\ S\ cm^{-1}$.

An important factor affecting the conductivity of these complexes is the bandgap. Density functional calculations designed to probe the electronic structure of $[PcRuL]_n$ polymers with bridging ligands pyz, tri, tz, bpy, and bpyac showed that the valence bands of these polymers consist of contributions from the macrocycle and a significant contribution from the Ru d_{xy} orbitals [130]. The conduction band, in contrast, is composed of orbitals from the macrocycle and the bridging ligands with the notable exception of the ligand tz, where the conduction band is formed by orbitals from the tz π system exclusively. The calculated band gap for the polymer with tz bridging ligands is significantly smaller than the other calculated bandgaps, which is reflected in its higher measured conductivity. The trend in the calculated bandgaps is consistent with the trend in the experimental conductivity data. Thus, in general, selection of bridging ligands with low-lying LUMOs and metallomacrocycles with high-lying HOMOs should lead to increased conductivity [131].

Substituents on the central ring of the bridging ligands may also significantly affect the conductivity. For example, in the case of the dib series of complexes, inclusion of alkyl or chloro groups on the central aromatic ring results in a significant decrease in conductivity.

Another trend evident in the data is that doping with iodine or hydrogen chloride results in an increase in conductivity. The trend is consistent throughout the series of polymers incorporat-

Table 5
Conductivity data for pressed polymer powders

[PcRuL]$_n$	Ligand	σ (S cm^{-1})	References
[PcRu]		2×10^{-5}	[41]
[2,3-NcRu]		3×10^{-4}	[98]
[PcRu(PhCN)$_2$]		3×10^{-11}	[32,64]
[PcRu(dib)]$_n$		3×10^{-6}	[32,64]
[PcRu(dib)I]$_n$		1×10^{-3}	[64]
[PcRu(dib)I$_{1.5}$]$_n$		4×10^{-3}	[64]
[PcRu(dib)I$_2$]$_n$		1×10^{-2}	[64,126]
[PcRu(Medib)]$_n$	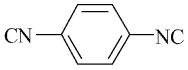	9×10^{-8}	[69]
[PcRu(Me$_2$dib)]$_n$		1×10^{-8}	[69]
[PcRu(Me$_4$dib)]$_n$		1×10^{-7}	[41]
[PcRu(Cl$_4$dib)]$_n$		1×10^{-7}	[41]
[PcRu(F$_4$dib)]$_n$		1×10^{-3}	[127,128]
[PcRu(*t*Bu$_2$dib)]$_n$		5×10^{-9}	[69]
[PcRu{(C$_8$H$_{17}$)$_2$dib}]$_n$		2×10^{-9}	[69]
[PcRu{(C$_{10}$H$_{21}$)$_2$dib}]$_n$		$<1 \times 10^{-12}$	[69]
[PcRu(pyz)$_2$]		$1–2 \times 10^{-11}$	[32,63]
[PcRu(pyz)]$_n$		1×10^{-7}	[32]
[PcRu(pyz)]$_n$		1×10^{-5}	[63]
[PcRu(pyz)I$_{0.7}$]$_n$		7×10^{-3}	[64]
[PcRu(pyz)I$_{1.3}$]$_n$		2×10^{-2}	[64]
[PcRu(pyz)I$_2$]$_n$		2×10^{-2}	[64]
[{(*t*Bu)$_4$Pc}Ru(pyz)]$_n$		7×10^{-8}	[77]
[2,3-NcRu(pyz)]$_n$		7×10^{-3}	[98]
[PcRu(tz)$_2$]		1×10^{-11}	[42,66,127–129]
[PcRu(tz)]$_n$		1×10^{-2}	[42,66,127–129]
[PcRu(Cl$_2$tz)]$_n$		$3–4 \times 10^{-3}$	[107,127,128]
[{(*t*Bu)$_4$Pc}Ru(tz)]$_n$		1×10^{-6}	[77]
[2,3-NcRu(tz)]$_n$		4×10^{-2}	[98]
[PcRu(Me$_2$tz)]$_n$		4×10^{-3}	[43,127]
[PcRu(dabco)]$_n$		1×10^{-9}	[77]
[{(*t*Bu)$_4$Pc}Ru(dabco)]$_n$		$<10^{-12}$	[77]
[2,3-NcRu(dabco)]$_n$		1×10^{-4}	[77]
[PcRu(dabco)·1.4CHCl$_3$]$_n$		10^{-10}	[127,128]
[PcRu(bpy)]$_2$	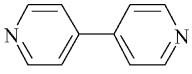	1×10^{-11}	[32]
[PcRu(bpy)]$_n$		2×10^{-8}	[32,77]
[{(*t*Bu)$_4$Pc}Ru(bpy)]$_n$		1×10^{-10}	[77]
[2,3-NcRu(bpy)]$_n$		3×10^{-5}	[77]
[PcRu(ppd)]$_n$	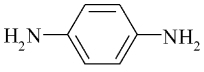	5×10^{-9}	[127,128]
[PcRu(ppd)·2H$_2$O]$_n$		4.6×10^{-9}	[67]
[PcRu(ppd)I$_{1.2}$]$_n$		2.1×10^{-3}	[67]
[PcRu(ppd)·(HCl)$_2$·3H$_2$O]$_n$		4.0×10^{-6}	[67]
[PcRu(ppd)·(HCl)$_{1.5}$·2H$_2$O]$_n$		5.0×10^{-5}	[67]
[PcRu(datz)]$_n$	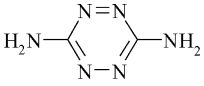	$3–4 \times 10^{-3}$	[107,127,128]
[{(*t*Bu)$_4$Pc}Ru(datz)]$_n$		3×10^{-8}	[77]
[{(*t*Bu)$_4$Pc}Ru(Me$_2$pyNC)]$_n$	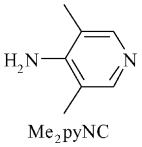	2×10^{-10}	[77]
[2,3-NcRu(Me$_2$pyNC)]$_n$		1×10^{-5}	[77]

Table 5 (*Continued*)

$[PcRuL]_n$	Ligand	σ (S cm^{-1})	References
$[2,3\text{-NcRu(dia)}]_n$	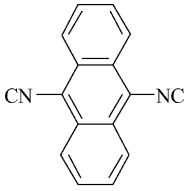 dia	2×10^{-4}	[77]
$[PcRu(bpyac)]_n$	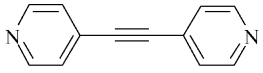 bpyac	4×10^{-7}	[64]
$[PcRu(bpyac)I_{1.2}]_n$		3×10^{-3}	[64]
$[PcRu(daf)]_n$	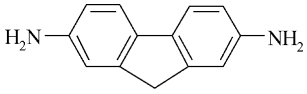 daf	3.0×10^{-8}	[67]
$[PcRu(daf)I_{1.3}]_n$		5.0×10^{-4}	[67]
$[PcRu(apy)]_n$	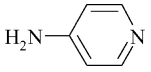 apy	2.9×10^{-4}	[67]
$[PcRu(apy)I_{3.7}\cdot H_2O]_n$		5.0×10^{-4}	[67]
$[PcRu(tri)_2]$	 tri	1×10^{-9}	[107,127,128]
$[PcRu(tri)]_n$		2×10^{-4}	[107,127,128]
$[PcRu(triest)]_n$	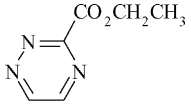 triest	5×10^{-4}	[107]
$[PcRu(3\text{-atri})]_n$	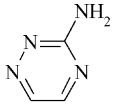 3-atri	8×10^{-4}	[107]
$[PcRu(5\text{-atri})]_n$	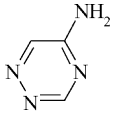 5-atri	5×10^{-5}	[107]
$[PcRu\{(CN)_2C_6F_4\}]_n$	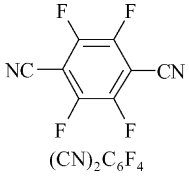 $(CN)_2C_6F_4$	1×10^{-3}	[128]
$[PcRu(CN)_2(CH)_2]_n$		3×10^{-2}	[128]
HO–$[PcRuO]_n$–H		1×10^{-2}	[70]

ing dib, pyz, bpyac, ppd, daf and api bridging ligands. Oxidation by iodine may take place either on the bridging ligand or macrocycle depending on the ligand used [67]. For example, in the ppd systems, the ligand is oxidized by I_2 while in the apy system, the IR spectrum is consistent with macrocycle oxidation. In either case, carrier density appears to increase upon oxidative doping leading to increased conductivities.

Including bulky *t*-butyl groups on the periphery of the Pc macrocycle invariably leads to a decrease in conductivity, as shown by comparison of the polymers $[PcRuL]_n$ with $[\{2,9,16,23\text{-}(t\text{Bu})_4\text{Pc}\}\text{RuL}]_n$. This conductivity decrease is presumably due to steric considerations hindering favourable ring interactions. Interestingly, the polymers formed from naphthalocyanine complexes are more conductive than the phthalocyanine analogs. For example $[2,3\text{-NcRu(L)}]_n$ has a higher conductivity than $[PcRu(L)]_n$ where L = pyz, tz, dabco and bpy. Calculations have shown [132] that upon proceeding from the Pc to Nc ring system, the HOMO is destabilized leading to a smaller HOMO-LUMO gap in Nc systems and a predicted increase in conductivity, which is seen in the experimental data tabulated here.

All of the tabulated polymers have Ru metal centres formally in the +2 oxidation state with the exception of the polymer HO–$[PcRuO]_n$–HO reported by Capobianchi et al., which has Ru^{IV} metal centres and a high conductivity. It is suggested that in this system, charge transfer may occur through dπ(Ru)–pπ(O)–dπ(Ru) linkages [70].

4. Applications

4.1. RuPc as thin films

4.1.1. Thin films by evaporation and vacuum deposition

Thin films of ruthenium phthalocyanine have been prepared on Ag, Pt, Cu, Au, Al_2O_3, AgI [133,134] SiO_2, and even adhesive tape substrates [124]. Surface oxides (RuO_x) on PcRu films readily form upon contact with air and/or water. The RuO_x forms a highly conductive layer that covers the underlying PcRu layer. Photovoltaic devices based on thin films of PcRu show improved performance upon oxygen doping, and this was attributed to the increased conductivity of the PcRu layer [135]. Vacuum evaporation of $[(PcRu)_2]$ (prepared *in situ* by thermal decomposition of $[PcRu(py)_2]$) under careful working conditions reproducibly gave oxygen-free, uniform films [124]. In contrast to most phthalocyanine thin films, the amorphous films could not be made crystalline by post-annealing. Schmeisser et al. [106] prepared thin films of PcRu on Ag substrates using Knudsen evaporation. As well as the expected species, Ru^0 was detected by XPS. However, in a later investigation, no evidence of metallic Ru in films prepared by evaporation could be found using XPS [100].

The application of metallophthalocyanines as gas sensing materials has received some attention [136,137]. Gases such as NO_2 and O_3 are able to induce significant changes in PcRu electronic properties, which can be exploited for gas sensing applications. The interaction between films of $[(PcRu)_2]$ and gaseous nitrogen oxides (NO_x) was studied by energy dispersive X-ray reflectometry (EDXR) [138,139] and conductivity [140]. The interaction was not restricted to the film surface; changes in thickness and roughness indicate that the gas is initially adsorbed onto the film surface, followed by intercalation of the gas molecules into the bulk film. Further EDXR studies revealed that the gas absorption/desorption process occurs in two steps [141]. The first step, un-influenced by initial film thickness, involves a rapid growth in film thickness as gas molecules absorb onto the film surface. The film roughness increases until the end of this process. In the second step, the film roughness remains constant while a slower increase in film thickness is observed as gas molecules interact with the bulk film. These processes are thermally reversible; heating at 130 °C reverses the second process while heating to 200 °C returns the film to its original thickness. The two-step mechanism was confirmed by *in situ* EDXR monitoring of the absorption/desorption process [142]. Using morphological monitoring of $[(PcRu)_2]$ thin films by EDXR, NO_2 concentrations as low as 10 ppm have been detected [143].

4.1.2. Langmuir–Blodgett thin films

Stable Langmuir–Blodgett films were prepared using the tetra-crown-substituted complex $[\{(15\text{-crown-}5)_4\text{Pc}\}\text{Ru(CO)(MeOH)}]$ [144]. The phthalocyanine molecules were stacked in the film with the macrocyclic planes 25° to the surface normal. Compared to the bulk, the electronic spectrum displays a bathochromic shift of the Q band, a hypsochromic shift of the S band, and a new (unassigned) absorption band at 880 nm. The film displays high electrochemical stability and electroactivity.

4.1.3. Self-assembled monolayers

Self-assembled monolayers (SAMs) incorporating PcRu were prepared on gold substrates using a two-step process [48]. A monolayer of 1,4-diisocyanobenzene (where the molecules lie perpendicular to the gold surface leaving free isocyanide groups) was immersed in a solution of $[PcRu(PhCN)_2]$. Labile benzonitrile ligands are displaced by the surface-bound isocyanate groups to give a monolayer of PcRu grafted onto the 1,4-diisocyanobenzene monolayer via coordinative bonds. Similarly, Li et al. prepared PcRu SAMs on modified silver surfaces [145,146]. Silver substrates were modified with monolayers of 4-mercaptopyridine, 1,4-bis[2-(4-pyridyl)ethenyl]-benzene or terephthalonitrile and PcRu was coordinated to the surface by immersion of the substrate in a ruthenium phthalocyanine solution. The nature of the second axial ligand, if any, or if the dimeric nature of $[(PcRu)_2]$ was retained, was not reported.

Scheme 10 shows a preparative method whereby ruthenium phthalocyanine complexes bearing ligands with functional CHO groups are reacted with functionalised substrates (gold or silicon dioxide) [49]. Silicon dioxide surfaces functionalized with 3-aminopropylmethyldiethoxysilane or gold surfaces functionalized with 4-aminophenyl disulfide possess amino groups that form imine linkages with the $[PcRu(4\text{-pyridinecarboxaldehyde})_2]$ molecules. A second adlayer is produced by first reacting the remaining 4-pyridinecarboxaldehyde ligand with 4′-amino-4-stilbazole followed by coordination of 5,10,15,20-tetraphenyl-21H,-23H-porphine $cobalt^{II}$ (CoTPP).

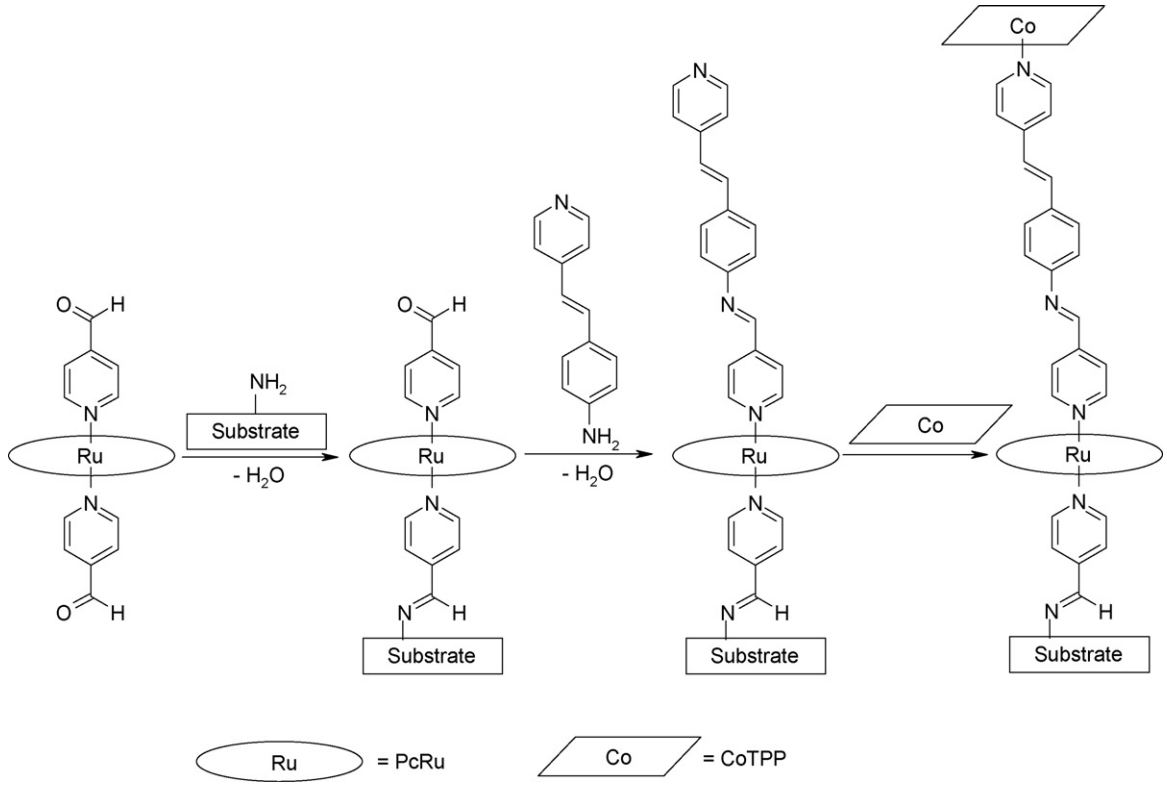

Scheme 10. Multilayer formation using a reactive substrate and axial ligand [49].

In a similar fashion, monolayers incorporating two PcRu units were prepared using a pyridine-functionalised substrate [50]. Glass slides were treated with (1-(3-triethoxysilyl)propyl)-3-(pyridine-4-methyl)-urea, to give pyridine-functionalized surfaces. Immersion of this substrate in a solution of [PcRu(PhCN)$_2$] gave a stable PcRu monolayer with a ligated benzonitrile at the monolayer surface. A second macrocyclic layer was added using two methods. The first involved the displacement of the remaining benzonitrile ligand with a bidentate ligand followed by complexation of a second layer. Using pyrazine as a bidentate ligand, a second PcRu layer was added; using 4,4′-bipyridine, a second macrocyclic layer of 5,10,15,20-tetraphenyl-21*H*,23*H*-porphinecobalt(II) was added. The second method for bilayer formation involved displacement of the monolayer benzonitrile ligand with [PcRu(bpy)$_2$] to give the second PcRu layer in one step. Using either method, the second macrocyclic layer was less dense than anticipated, possibly due to hindrance of coordination sites caused by some disorder in the monolayer.

4.2. Catalysis

Ruthenium phthalocyanine complexes have been investigated in a range of catalytic applications. Although a significant amount of research investigating metallophthalocyanines as catalysts has focused on cobalt and iron derivatives, ruthenium phthalocyanine complexes show a similar level of catalytic versatility in many cases [147].

4.2.1. Oxidation catalysts

Ruthenium phthalocyanine complexes catalysed the oxidation of cyclohexane to cyclohexanone and cyclohexanol by *t*-butylhydroperoxide [86,87,148]. Reactions using [(PcRu)$_2$] had low turnover frequencies and the catalyst decomposed after only 5 h. Using [(F_{16}Pc)Ru] increased the turnover frequency and stability, but due to the formation of oxo-bridged dimers (detected by UV–vis and IR spectroscopy) turnover frequencies were still low. Encapsulation of [F_{16}PcRu] in zeolite cages prevented dimer formation and significantly improved the turnover frequency as well as selectivity toward cyclohexanone production. [Cl_{16}PcRu] immobilised in molecular sieves displayed a low turnover frequency in cyclohexane oxidation reactions [90]. Synthesis of the commercially important adipic acid via the oxidation of cyclohexane, cyclohexanol and cyclohexanone using tetra-sulfo-metallophthalocyanines as catalysts was investigated [149]. The reactions were performed in water with potassium monopersulfate as oxidiser. [{2,9,16,23-($NaSO_3$)$_4$Pc}Ru] gave superior yields and selectivity for adipic acid formation from cyclohexanone, cyclohexanol and cyclohexane. Oxidation of *n*-hexane was also examined by molecular sieve encased [F_{16}PcRu], [90] however the catalyst lost activity after 1 day, tentatively postulated as the result of pore blockage by polar reaction products.

Zeolite-encased PcRu showed activity in the partial oxidation of methane to methanol in a fixed-bed flow reactor [30]. Methane conversion was low (4.8%) and CO_2 was a major by-product. At higher temperature methanol yield decreased,

presumably due to PcRu decomposition. Only CO_2 and H_2O were produced using ruthenium tetra-sulfo-phthalocyanine on a magnesium oxide support.

Ruthenium tetra-sulfo-phthalocyanine is an effective catalyst in the oxidation of various α-chloro-alkenes [74] and chlorinated phenols [73], and the oxidation of C_1–C_4 alcohols [150] with hydrogen peroxide and/or monopersulfate in neutral and acidic aqueous media. α-Chloro-alkenes underwent ketonisation, oxidative cleavage, epoxidation and dehydrochlorination depending on the substrate. The reaction of chlorinated phenols is rapid and complete, with HCl and CO_2 as the main products. Oxidation of primary alcohols gave carboxylic acids while secondary alcohols were initially oxidised to the corresponding ketones, however further oxidation produced esters (via Baeyer–Villiger oxidation), which were hydrolysed under the reaction conditions. The final products consisted mainly of carboxylic acids. [{2,9,16,23-$(NaSO_3)_4$Pc}Ru] was determined to be a pre-catalyst in the reactions, with oxidative degradation of the macrocycle leading to the catalytically active species. A mechanism for the formation of the active species has been tentatively assigned [151] whereby peroxide oxidises a *meso* nitrogen of the phthalocyanine ring. The resulting mono-nitrogen-oxide loses ammonia and 3-sulfophthalimide to form the catalytically active, tridentate diamagnetic species. In alkaline environments, the above reaction and therefore catalysis does not occur [74].

Diesel fuel production includes the desulfurization of sulphur-containing compounds. Of the polycyclic aromatic sulphur hydrocarbons found in crude oils, dibenzothiophene analogues are among the most abundant. In a range of tetra-sulfo-metallophthalocyanines, the ruthenium complex was the most effective in the catalytic oxidation and desulfurisation of dibenzothiophene with monopersulfate at ambient temperatures [152]. The final products included carbon dioxide, oxalic acid, sulfuric acid and benzoic acid.

[$(PcRu)_2$] in thf was found to activate dioxygen, thus its catalytic activity in the selective oxidation of terminal olefins to the corresponding ketones was assessed [37]. [$(PcRu)_2$] with [$PdCl_2(PhCN)_2$] as olefin activator catalyzed the oxidation of 1-octene to 2-octanone, and oxidation of 1-decene to 2-decanone. [$PcRu(dmso)_2$] and [$PcRu(py)_2$] showed no catalytic activity as the axial ligands blocked O_2 activation.

[$(PcRu)_2$]-modified electrodes effectively catalysed the four electron oxidation of N_2H_4 to N_2 at pH > 9 [147]. The initial step is a one-electron oxidation of [$(RuPc)_2$] to [$(Ru^{III}Pc^{2-})(Ru^{II}Pc^{2-})]^+$. Coordination of N_2H_4 to Ru^{III} and proton abstraction by OH^- produces a coordinated N_2H_3 species. Rapid consecutive losses of protons and electrons yield N_2. The absence of catalytic activity below pH 9 is assigned the inability of the solution to deprotonate the coordinated hydrazine. The electrode was shown to be an excellent N_2H_4 detector.

Hydroxylamine is an important intermediate in the oxidation of ammonia and its electrocatalytic oxidation is of interest. [$(PcRu)_2$]-modified electrodes were effective in the electrocatalytic oxidation of NH_2OH [153] to N_2O in the pH range 9–13. Hydroxylamine, coordinated to $[(Ru^{III}Pc)(Ru^{II}Pc)]^+$, loses a proton and an electron to form HNO. Ejection of HNO into solution, followed by dimerization, yields N_2O.

[$PcRu(dmso)_2$] on a glassy carbon electrode shows catalytic behaviour towards the oxidation of the amino acid cysteine to the corresponding disulfide, cystine [154]. The mechanism involves phthalocyanine ring oxidation and formation of the dimeric π-cation, which in turn oxidises cysteine. The lack of catalytic activity of [$PcRu(py)_2$] is explained by its inability to form dimers due to the relatively non-labile pyridine ligand.

4.2.2. Reduction catalysts

In the catalytic reduction of NO with CO, zeolites containing PcRu were more efficient than those containing $[RuNO(NH_3)_4(OH)]^{2+}$, presumably due to the higher reactivity of coordinatively unsaturated PcRu [29]. In comparison to other metallophthalocyanines, ruthenium phthalocyanine showed low catalytic activity in the reduction of NO by CO [26–28] although zeolite encased PcRu did show good stability at 200–300 °C in the catalytic cycle [26].

N_4 macrocyclic metal complexes have been explored as alternatives to platinum in the catalytic reduction of oxygen. In this context, oxygen is reduced in a two electron process to hydrogen peroxide, which may undergo further two electron reduction to water [111]. In a series of metallophthalocyanine complexes adsorbed to carbon supports [155], the ruthenium example showed mid-range activity in the electrocatalytic reduction of oxygen to water. Heat treatment of the catalyst greatly increased its activity [156]. Reduction of oxygen to hydrogen peroxide with a [$(PcRu)_2$] modified electrode occurs in a narrow potential range regardless of pH, a behaviour generally exhibited by metallophthalocyanines [111]. However, reduction of hydrogen peroxide can occur by three different processes depending on the solution pH [111]. This behaviour is unique to [$(PcRu)_2$] and is believed to be a result of the formation of three different electrode surfaces. The first process, observed between pH 1–7, occurs at the most negative potentials, while a second process occurs between pH 3–10 at less negative potentials. Interestingly between pH 3–8 these two processes occur simultaneously and may represent two sequential one-electron reductions of hydrogen peroxide. At pH > 10, a third process occurs at a potential more positive than that of oxygen reduction, thus reduction of oxygen directly to water is observed at pH above 10. Decomposition of hydrogen peroxide catalysed by a PcRu/C electrode was found to be slow in acidic environments, but much more rapid in alkaline environments [155].

Ruthenium phthalocyanine did not catalyze the simultaneous electroreduction of CO_2 and NO_2^- to urea [157]; catalyzing the reduction of NO_2^- but not CO_2. [$(PcRu)_2$] modified graphite electrodes were effective in the electroreduction of NO_2^- in pHs above 4 [158]. At low NO_2^- concentrations NH_3 was the main product, while at high concentrations N_2O and NH_2OH were also produced. [$PcRu]_2$ was ineffective in the simultaneous electroreduction of CO_2 and NO_3^- [159]. The catalyst did not catalyse the reduction of NO_3^-, a property shared by all metallophthalocyanines tested.

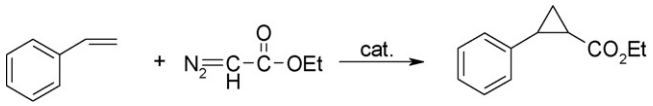

Scheme 11. Cyclopropanation of styrene with ethyl diazoacetate.

4.2.3. Hydrogenation and cyclopropanation catalysts

The hydrogenation of compounds containing heteroatoms to separable gases (H_2S, H_2O, NH_3) is used in the processing of coal liquids. Ruthenium phthalocyanine complexes have been examined in the search for cheaper and milder methods of hydrogenation [160]. Interestingly, compounds with two or three N-heterocyclic rings, e.g. quinoline, were hydrogenated but other N-containing compounds were not, e.g. aniline, pyridine.

Cyclopropanation of alkenes catalyzed by metallophthalocyanine complexes (Scheme 11) has been investigated [161] with ruthenium phthalocyanine examples amongst the most efficient. Substitution of the macrocycle periphery with electron-withdrawing substituents increased the catalytic performance with [F_{16}PcRu] giving the highest cyclopropanation yields of the metallophthalocyanines tested. [F_{16}PcRu] also catalyzed the cyclopropanation of various substituted styrenes with yields ranging from 62 to 91%.

4.3. Photodynamic therapy

Photodynamic therapy (PDT) involves the use of a dye combined with irradiation by light to cause cell and tissue destruction in specific regions of living organisms [162,163]. The regions targeted are often cancerous lesions. Pc and Nc complexes have been investigated as PDT dyes because of their strong optical absorption properties at an appropriate wavelength. An effective PDT dye should absorb light in a region where tissue is most transparent; this corresponds to an optical window in the wavelength range 650–1400 nm. However, the mechanism of PDT requires that light has sufficient energy to evolve singlet state oxygen, which is believed to be the species responsible for cell death and tissue destruction [162,163]. This requires a wavelength <800 nm. The intense Q-band absorption of Pc and Nc compounds generally falls the desired wavelength range 650–800 nm.

Generation of singlet oxygen by PDT dyes may work by two mechanisms. Firstly, a photoexcited dye may interact with an intermediate molecule leading to electron or hydrogen transfer, and the excited intermediate may then react further with oxygen to generate the singlet oxygen species. Secondly, a photoexcited dye may react directly with O_2 to generate singlet oxygen. Dye stability must also be considered as it is important that the rate of photobleaching (degradation that occurs from light exposure) is within acceptable limits. Furthermore, because PDT dyes must operate in the body, they should be water-soluble.

The complex K_2[PcRu(TPPMS)$_2$], where TPPMS = $Ph_2P(3\text{-}C_6H_4SO_3^-)$, Fig. 9, was prepared [21] and has good water solubility. The Q-band has maximum intensity at 652 nm with a molar absorptivity of $8.8 \times 10^4\ M^{-1}\ cm^{-1}$. Experiments comparing its cytotoxicity in the dark and under illumination to HeLa

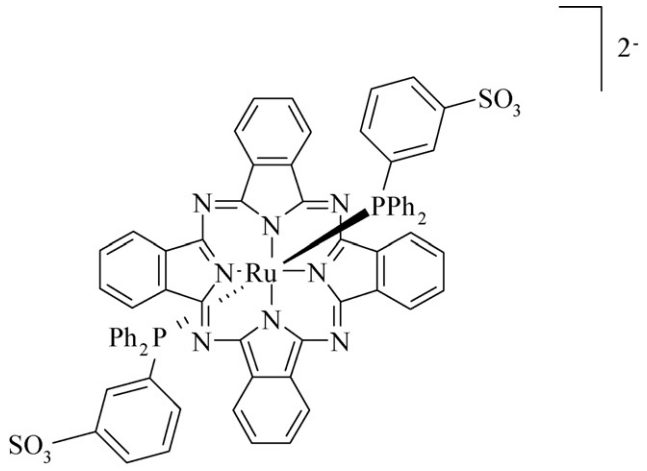

Fig. 9. The water soluble complex K_2[PcRu(TPPMS)$_2$].

tumour cells *in vitro* showed that while the complex was effectively non-toxic at concentration greater than 10^{-5} M in the dark, 50% of the cells were killed using a 10^{-6} M concentration in conjunction with illumination at 650 nm [22]. PDT experiments in mice showed that radiation-induced fibrosarcoma tumour cells could be completely destroyed using this complex [164]. The complex photobleaches under aerobic and anaerobic conditions and produces only very small amounts of singlet oxygen upon irradiation. The suggested mechanism of action is most likely to involve an electron transfer event involving an intermediate species, which was not elucidated [164].

Water soluble complexes of the type [NcRuL$_2$] were prepared where L = 3-pyridinesulfonic acid, nicotinic acid, pyrazinic acid, triphenylphosphine-*m*-disulfonic acid, taurine, β-alanine, and D-glucamine [99]. Q-band absorptions in the wavelength range 716–760 nm were very intense with molar absorptivity coefficients in the order of $2 \times 10^5\ M^{-1}\ cm^{-1}$. *In vitro* toxicity tests showed that each of the complexes was photoactive in the micromolar range against HeLa cells. The complexes photobleach under aerobic and anaerobic conditions with the aerobic rate approximately ten times that of the anaerobic rate.

4.4. Dye-sensitised solar cells

The dye-sensitized solar cell (DSC) has been investigated as a photovoltaic device with possible production cost advantages over conventional silicon-based cells. It generally consists of two conducting glass electrodes, one of which is coated with a porous layer of titanium dioxide nanoparticles to which a sensitizing dye is adsorbed *via* functional groups (see Fig. 10). Because this layer has a very large surface area, a high concentration of surface-bound dye molecules can be achieved. An electrolyte solution containing a redox mediator (for example, I_2/I_3^-) fills the space between the two electrodes. The role of the redox mediator is to reduce the oxidized dye after electron transfer has occurred from the photoexcited dye to the titanium dioxide. Reviews of the DSC may be found in reference [165].

Several properties have been identified for effective sensitizing dyes: (i) efficient absorption of incident solar photons,

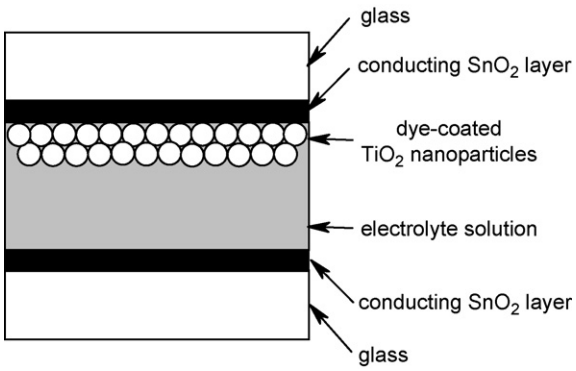

Fig. 10. Schematic diagram of a DSC.

(ii) the energy of the photoexcited state must be sufficient to allow electron injection from the dye into the conduction band of titanium dioxide, (iii) good overlap of dye-based orbitals with orbitals on the semi-conductor for efficient electron transfer, (iv) the oxidation potential of the dye must allow the redox mediator to reduce the oxidized dye after electron transfer to the semiconductor has occurred, and (v) the dye must be stable over many redox cycles under solar irradiation.

Ruthenium phthalocyanine complexes have spectral, electronic, photoelectrochemical and redox properties that satisfy the above criteria and have therefore been targeted for investigation. Nazeeruddin et al. report the first use of a ruthenium phthalocyanine complex as a sensitiser in a nanocrystalline TiO_2 DSC [166]. [{1,4,8,11,15,18,22,25-$(Me)_8$Pc}Ru(3,4-dicarboxypyridine)$_2$] was anchored to the titanium dioxide nanoparticle electrode via carboxylic acid groups. The resulting photovoltaic device had an incident photon to current conversion efficiency (IPCE) of over 60% in the near IR region (660 nm).

Yanagisawa et al. prepared two ruthenium phthalocyanine dyes as DSC sensitisers [23]. The first, [PcRu(4-carboxypyridine)$_2$] showed an IPCE of 21% at 640 nm and an overall conversion efficiency (η) of 0.61%, one of the highest recorded for a phthalocyanine based solar cell. A device using the peripherally substituted [{2,3,9,10,16,17,23,24-$(C_5H_{11}O)_8$-Pc}Ru(4-carboxypyridine){4-(2-ethoxy)ethyloxycarbonylpyridine}] yielded an IPCE of 6.6% at 640 nm and a conversion efficiency of 0.58%. The differences are believed to arise from the additional carboxylic acid group in [PcRu(4-carboxylpyridine)$_2$] and the effect of peripheral pentoxy groups.

Anchoring of a ruthenium phthalocyanine complex to titanium dioxide has also been achieved via carboxylic acid groups attached to the macrocycle periphery. [{2,3,9,10,16,17-$(C_5H_{11}O)_6$-23,24-{(4-carboxy)phenoxy}$_2$Pc}Ru(4-Mepy)$_2$] (see Scheme 6 in Section 2.2.1) was anchored to titanium dioxide with the macrocyclic plane assumed to be perpendicular to the semiconductor surface [89]. The 4-methylpyridine axial ligands serve to prevent aggregation. An IPCE of 23% and conversion efficiency of 0.40% were recorded for DSCs incorporating this complex. The Zn analogue, lacking the axial picoline ligands, exhibited poorer efficiency, believed to be the result of aggregation.

[PcRu(4-carboxypyridine)$_2$] was found by X-ray and UV photoemission spectroscopy to have HOMO and LUMO energies similar to those of *cis*-bis(4,4′-dicarboxy-2,2′-bipyridine)-bis-(isothiocyanato)-ruthenium(II) [Ru(dcbpy)$_2$(NCS)$_2$], a highly efficient and successful DSC sensitiser [167]. The oxidation potentials for the ground and excited states are also similar for the two complexes. The energy difference between the [PcRu(4-carboxypyridine)$_2$] LUMO and the TiO_2 conduction band was favourable for electron transfer to occur between the two bands, although it was not as favourable as that of [Ru(dcbpy)$_2$(NCS)$_2$].

The use of thin films of ruthenium phthalocyanine in photovoltaic devices has been investigated [135]. Using indium-doped tin oxide (ITO) on glass as a substrate, fullerene (C_{60}), PcRu and Ag layers were deposited. The resulting device had high series resistance and strong recombination at the C_{60}/PcRu interface, however encouraging photocurrent values were obtained. The performance was reduced by exposure of the PcRu film to N_2 prior to deposition of Ag. This was attributed to a decrease in the PcRu film conductivity as a result of no O_2 doping.

5. Conclusions

The synthesis and properties of ruthenium phthalocyanine complexes have been extensively investigated while ruthenium naphthalocyanine complexes remain less studied. Complexes incorporating a variety of axial ligands and peripheral substituents have been reported although from the vast range of potential axial ligands, only a relatively small number have been explored. Given that many ruthenium phthalocyanine complexes exhibit interesting and potentially useful properties, we anticipate that many new examples will be forthcoming.

References

[1] C.C. Leznoff, A.B.P. Lever (Eds.), Phthalocyanines: Properties and Applications, VCH, New York, 1989.
[2] K. Kasuga, M. Tsutsui, Coord. Chem. Rev. 32 (1980) 67.
[3] A.L. Thomas, Phthalocyanine Research and Applications, CRC Press, Boca Raton, Fla, 1990.
[4] K.M. Kadish, K.M. Smith, R. Guilard (Eds.), The Porphyrin Handbook, vol. 16–20, Academic Press, New York, 2003.
[5] G. Wilkinson, R.D. Gillard, J.A. McCleverty (Eds.), Comprehensive Coordination Chemistry: The Synthesis, Reactions, Properties & Applications of Coordination Compounds, Pergamon Press, Oxford, 1987.
[6] J.A. McCleverty, T.J. Meyer (Eds.), Comprehensive Coordination Chemistry. II: From biology to nanotechnology, vol. 5, Elsevier Ltd., Oxford, 2004.
[7] P.C. Krueger, M.E. Kenney, J. Inorg. Nucl. Chem. 25 (1963) 303.
[8] I.M. Keen, B.W. Malerbi, J. Inorg. Nucl. Chem. 27 (1965) 1311.
[9] I.M. Keen, Platinum Met. Rev. 8 (1964) 143.
[10] B.D. Berezin, G.V. Sennikova, Dokl. Akad. Nauk 159 (1964) 117.
[11] S. Omiya, M. Tsutsui, E.F. Meyer Jr., I. Bernal, D.L. Cullen, Inorg. Chem. 19 (1980) 134.
[12] L.J. Boucher, P. Rivera, Inorg. Chem. 19 (1980) 1816.
[13] M.M. Doeff, D.A. Sweigart, Inorg. Chem. 20 (1981) 1683.
[14] F. Pomposo, D. Carruthers, D.V. Stynes, Inorg. Chem. 21 (1982) 4245.
[15] K.R. Seddon, Coord. Chem. Rev. 41 (1982) 79.
[16] A. Shaabani, F. Bahadoran, A. Bazgir, N. Safari, Iran. J. Chem. Chem. Eng. 18 (1999) 104.

[17] A. Shaabani, F. Bahadoran, N. Safari, Indian J. Chem. Sect. A 40A (2001) 195.
[18] D. Villemin, M. Hammadi, M. Hachemi, N. Bar, Molecules 6 (2001) 831.
[19] N.P. Farrell, A.J. Murray, J.R. Thornback, D.H. Dolphin, B.R. James, Inorg. Chim. Acta 28 (1978) L144.
[20] D. Dolphin, B.R. James, A.J. Murray, J.R. Thornback, Can. J. Chem 58 (1980) 1125.
[21] G.E. Bossard, M.J. Abrams, M.C. Darkes, J.F. Vollano, R.C. Brooks, Inorg. Chem. 34 (1995) 1524.
[22] M.J. Abrams, Platinum Met. Rev. 39 (1995) 14.
[23] M. Yanagisawa, F. Korodi, J. He, L. Sun, V. Sundstrom, B. Akermark, J. Porphyrins Phthalocyanine 6 (2002) 217.
[24] A. Bulatov, S. Knecht, L.R. Subramanian, M. Hanack, Chem. Ber. 126 (1993) 2565.
[25] A.G. Gabrielov, A.N. Zakharov, B.V. Romanovsky, O.P. Tkachenko, E.S. Shpiro, K.M. Minachev, Koord. Khim. 14 (1988) 821;
A.G. Gabrielov, A.N. Zakharov, B.V. Romanovsky, O.P. Tkachenko, E.S. Shpiro, K.M. Minachev, Engl. Trans. Sov. J. Coord. Chem. 14 (1988) 740.
[26] B.V. Romanovsky, A.G. Gabrielov, Mendeleev Commun. (1991) 14.
[27] B.V. Romanovsky, A.G. Gabrielov, J. Mol. Catal. 74 (1992) 293.
[28] B.V. Romanovsky, A.G. Gabrielov, Stud. Surf. Sci. Catal. 72 (1992) 443.
[29] E.S. Shpiro, G.V. Antoshin, O.P. Tkachenko, S.V. Gudkov, B.V. Romanovsky, K.M. Minachev, Stud. Surf. Sci. Catal. 18 (1984) 31.
[30] Y.W. Chan, R.B. Wilson Jr., Preprints of Papers - American Chemical Society, Division of Fuel Chemistry 33 (1988) 453.
[31] C.K. Choy, J.R. Mooney, M.E. Kenney, J. Magn. Reson 35 (1979) 1.
[32] W. Kobel, M. Hanack, Inorg. Chem. 25 (1986) 103.
[33] T. Nyokong, Polyhedron 12 (1993) 375.
[34] G. Rossi, M. Gardini, G. Pennesi, C. Ercolani, V.L. Goedken, J. Chem. Soc., Dalton (1989) 193.
[35] M. Hanack, J. Osio-Barcina, E. Witke, J. Pohmer, Synthesis (1992) 211.
[36] R. Polley, M. Hanack, Synthesis (1997) 295.
[37] A. Capobianchi, A.M. Paoletti, G. Pennesi, G. Rossi, R. Caminiti, C. Ercolani, Inorg. Chem. 33 (1994) 4635.
[38] M. Hanack, P. Vermehren, Chem. Ber. 124 (1991) 1733.
[39] A. Weber, T.S. Ertel, U. Reinohl, H. Bertagnolli, M. Leuze, M. Hees, M. Hanack, Eur. J. Inorg. Chem. (2000) 2289.
[40] U. Keppeler, W. Kobel, H.U. Siehl, M. Hanack, Chem. Ber. 118 (1985) 2095.
[41] U. Keppeler, M. Hanack, Chem. Ber. 119 (1986) 3363.
[42] U. Keppeler, S. Deger, A. Lange, M. Hanack, Angew. Chem. 99 (1987) 349;
U. Keppeler, S. Deger, A. Lange, M. Hanack, Engl. Trans. Angew. Chem. Int. Ed. 26 (1987) 344.
[43] M. Hanack, A. Lange, R. Grosshans, Synth. Met. 45 (1991) 59.
[44] M. Hanack, Y.G. Kang, Chem. Ber. 124 (1991) 1607.
[45] M. Hanack, S. Knecht, H.-J. Schulze, J. Organomet. Chem. 445 (1993) 157.
[46] H. Bertagnolli, A. Weber, W. Hoerner, T.S. Ertel, U. Reinoehl, M. Hanack, M. Hees, R. Polley, Inorg. Chem. 36 (1997) 6397.
[47] X. Yang, M. Kritikos, B. Akermark, L. Sun, J. Porphyrins Phthalocyanine 9 (2005) 248.
[48] V. Huc, J.-P. Bourgoin, C. Bureau, F. Valin, G. Zalczer, S. Palacin, J. Phys. Chem. B 103 (1999) 10489.
[49] V. Huc, M. Saveyroux, J.-P. Bourgoin, F. Valin, G. Zalczer, P.-A. Albouy, S. Palacin, Langmuir 16 (2000) 1770.
[50] V. Huc, F. Armand, J.P. Bourgoin, S. Palacin, Langmuir 17 (2001) 1928.
[51] S. Sievertsen, H. Schlehahn, H. Homborg, Z. Anorg. Allg. Chem. 619 (1993) 1064.
[52] S. Sievertsen, H. Schlehahn, H. Homborg, Z. Naturforsch., B: Chem. Sci. 49 (1993) 50.
[53] M. Czekalla, S. Sievertsen, H. Homborg, Z. Anorg. Allg. Chem. 621 (1995) 1205.
[54] M. Weidemann, H. Hueckstaedt, H. Homborg, Z. Anorg. Allg. Chem. 624 (1998) 846.
[55] M. Weidemann, H. Homborg, Z. Anorg. Allg. Chem. 622 (1996) 1182.
[56] S. Sievertsen, M. Weidemann, H. Huckstadt, H. Homborg, J. Porphyrins Phthalocyanine 1 (1997) 379.
[57] M. Weidemann, H. Homborg, Z. Anorg. Allg. Chem. 622 (1996) 1705.
[58] S. Sievertsen, M. Weidemann, O. Tsantzi-Krause, H. Homborg, Z. Anorg. Allg. Chem. 621 (1995) 1567.
[59] M. Weidemann, S. Sievertsen, H. Homborg, Z. Anorg. Allg. Chem. 624 (1998) 909.
[60] C. Ercolani, J. Jubb, G. Pennesi, U. Russo, G. Trigiante, Inorg. Chem. 34 (1995) 2535.
[61] A. Kienast, C. Bruhn, H. Homborg, Z. Anorg. Allg. Chem. 623 (1997) 967.
[62] A. Kienast, L. Galich, K.S. Murray, B. Moubaraki, G. Lazarev, J.D. Cashion, H. Homborg, J. Porphyrins Phthalocyanine 1 (1997) 141.
[63] M. Hanack, A. Datz, W. Kobel, J. Koch, J. Metz, M. Mezger, O. Schneider, H.J. Schulze, J. Phys. Colloque (1983) 633.
[64] M. Hanack, U. Keppeler, H.J. Schulze, Synth. Met. 20 (1987) 347.
[65] A. Weber, T.S. Ertel, U. Reinohl, M. Feth, H. Bertagnolli, M. Leuze, M. Hanack, Eur. J. Inorg. Chem. (2001) 679.
[66] M. Hanack, S. Deger, U. Keppeler, A. Lange, A. Leverenz, M. Rein, Synth. Met. 19 (1987) 739.
[67] M. Hanack, Y.G. Kang, Synth. Met. 48 (1992) 79.
[68] M. Hanack, A. Hirsch, S. Kamenzin, R. Thies, P. Vermehren, Synth. Met. 42 (1991) 2633.
[69] M. Hanack, S. Kamenzin, C. Kamenzin, L.R. Subramanian, Synth. Met. 110 (2000) 93.
[70] A. Capobianchi, G. Pennesi, A.M. Paoletti, G. Rossi, R. Caminiti, C. Sadun, C. Ercolani, Inorg. Chem. 35 (1996) 4643.
[71] N. Kobayashi, Coord. Chem. Rev. 219–221 (2001) 99.
[72] H. Przywarska-Boniecka, Rocz. Chem. 42 (1968) 1577.
[73] M. Bressan, N. d'Alessandro, L. Liberatore, A. Morvillo, Coord. Chem. Rev. 185–186 (1999) 385.
[74] M. Bressan, N. Celli, N. d'Alessandro, L. Liberatore, A. Morvillo, L. Tonucci, J. Organomet. Chem. 593–594 (2000) 416.
[75] M. Hanack, P. Vermehren, Synth. Met. 32 (1989) 257.
[76] M. Hanack, S. Knecht, E. Witke, P. Haisch, Synth. Met. 55 (1993) 873.
[77] S. Knecht, R. Polley, M. Hanack, Appl. Organomet. Chem. 10 (1996) 649.
[78] M. Hanack, S. Knecht, R. Polley, Chem. Ber. 128 (1995) 929.
[79] A.S. Dudnik, A.V. Ivanov, L.G. Tomilova, N.S. Zefirov, Russ. J. Coord. Chem. 30 (2004) 110.
[80] K. Durr, M. Hanack, J. Porphyrins Phthalocyanine 3 (1999) 224.
[81] M. Hanack, M. Hees, E. Witke, New J. Chem. 22 (1998) 169.
[82] Y.Y. Enakieva, Y.G. Gorbunova, S.G. Sakharov, A.Y. Tsivadze, Russ. J. Inorg. Chem. 47 (2002) 1815.
[83] Y.G. Gorbunova, L.A. Lapkina, A.Y. Tsivadze, J. Coord. Chem. 56 (2003) 1223.
[84] Y.G. Gorbunova, Y.Y. Enakieva, S.G. Sakharov, A.Y. Tsivadze, J. Porphyrins Phthalocyanine 7 (2003) 795.
[85] W. Eberhardt, M. Hanack, Synthesis (1998) 1760.
[86] K.J. Balkus Jr., M. Eissa, R. Levado, J. Am. Chem. Soc. 117 (1995) 10753.
[87] K.J. Balkus Jr., M. Eissa, R. Lavado, Stud. Surf. Sci. Catal. 94 (1995) 713.
[88] D. Christendat, M.-A. David, S. Morin, A.B.P. Lever, K.M. Kadish, J. Shao, J. Porphyrins Phthalocyanine 9 (2005) 626.
[89] M. Yanagisawa, F. Korodi, J. Bergquist, A. Holmberg, A. Hagfeldt, B. Akermark, L. Sun, J. Porphyrins Phthalocyanine 8 (2004) 1228.
[90] S. Ernst, M. Selle, Microporous Mesoporous Mater. 27 (1999) 355.
[91] B.D. Rihter, M.E. Kenney, W.E. Ford, M.A.J. Rodgers, J. Am. Chem. Soc. 112 (1990) 8064.
[92] G. Berber, A.N. Cammidge, I. Chambrier, M.J. Cook, P.W. Hough, Tetrahedron Lett. 44 (2003) 5527.
[93] A.N. Cammidge, G. Berber, I. Chambrier, P.W. Hough, M.J. Cook, Tetrahedron 61 (2005) 4067.
[94] Y.G. Gorbunova, Y.Y. Enakieva, S.G. Sakharov, A.Y. Tsivadze, Russ. Chem. Bull. 53 (2004) 74.
[95] Y.Y. Enakieva, Y.G. Gorbunova, S.E. Nefedov, A.Y. Tsivadze, Mendeleev Commun. (2004) 193.

[96] H.S. Nalwa, S. Kobayashi, A. Kakuta, MCLC S&T, Sect. B: Nonlinear Opt. 6 (1993) 169.
[97] S. Tai, S. Hayashida, N. Hayashi, US Patent 4,833,264 (1989).
[98] M. Hanack, R. Polley, Inorg. Chem. 33 (1994) 3201.
[99] J.F. Vollano, G.E. Bossard, S.A. Martellucci, M.C. Darkes, M.J. Abrams, R.C. Brooks, J. Photochem. Photobiol. B 37 (1997) 230.
[100] L. Alagna, A. Capobianchi, M.P. Casaletto, G. Mattogno, A.M. Paoletti, G. Pennesi, G. Rossi, J. Mater. Chem. 11 (2001) 1928.
[101] D.L. Ledson, M.V. Twigg, Inorg. Chim. Acta 13 (1975) 43.
[102] D. Guez, D. Markovitsi, M. Sommerauer, M. Hanack, Chem. Phys. Lett. 249 (1996) 309.
[103] P.A. Stuzhin, S.I. Vagin, M. Hanack, Inorg. Chem. 37 (1998) 2655.
[104] A. Antipas, J.W. Buchler, M. Gouterman, P.D. Smith, J. Am. Chem. Soc. 100 (1978) 3015.
[105] A.R. Gutierrez, Chem. Phys. Lett. 74 (1980) 293.
[106] D. Schmeisser, J. Pohmer, M. Hanack, W. Goepel, Synth. Met. 61 (1993) 115.
[107] J. Pohmer, M. Hanack, J. Osio Barcina, J. Mater. Chem. 6 (1996) 957.
[108] M. Hanack, S. Deger, A. Lange, Coord. Chem. Rev. 83 (1988) 115.
[109] M. Hanack, A. Gul, A. Hirsch, B.K. Mandal, L.R. Subramanian, E. Witke, Mol. Cryst. Liq. Cryst. 187 (1990) 625.
[110] C.-M. Che, T.-C. Lau, in: J.A. McCleverty, T.J. Meyer (Eds.), Comprehensive Coordination Chemistry. II: From Biology to Nanotechnology, vol. 5, Elsevier, Oxford, 2004, p. 734.
[111] M. Ebadi, C. Alexiou, A.B.P. Lever, Can. J. Chem 79 (2001) 992.
[112] N.G. Connelly, W.E. Geiger, Chem. Rev. 96 (1996) 877.
[113] G.M. Brown, F.R. Hopf, T.J. Meyer, D.G. Whitten, J. Am. Chem. Soc. 97 (1975) 5385.
[114] N. Kobayashi, S.-I. Nakajima, H. Ogata, T. Fukuda, Chem. Eur. J. 10 (2004) 6294.
[115] T. Nyokong, Z. Gasyna, M.J. Stillman, Inorg. Chim. Acta 112 (1986) 11.
[116] D.R. Prasad, G. Ferraudi, J. Phys. Chem. 86 (1982) 4037.
[117] D.R. Prasad, G. Ferraudi, Inorg. Chem. 22 (1983) 1672.
[118] D.R. Prasad, G. Ferraudi, Inorg. Chem. 21 (1982) 4241.
[119] M.K. Engel, in: K.M. Kadish, K.M. Smith, R. Guilard (Eds.), Porphyrin Handbook, vol. 20, Academic Press, New York, 2003, p. 1.
[120] A.V. Vannikov, A.D. Grishina, Y.G. Gorbunova, Y.Y. Enakieva, T.V. Krivenko, V.V. Savel'ev, A.Y. Tsivadze, Dokl. Phys. Chem. 403 (2005) 137.
[121] R. Caminiti, M.P. Donzello, C. Ercolani, C. Sadun, Inorg. Chem. 38 (1999) 3027.
[122] L. Alagna, A. Capobianchi, G. Pennesi, T. Prosperi, G. Rossi, J. Phys. IV 7 (1997) 1261.
[123] L. Alagna, A. Capobianchi, P. Marovino, A.M. Paoletti, G. Pennesi, T. Prosperi, G. Rossi, Inorg. Chem. 38 (1999) 3688.
[124] R. Caminiti, A. Capobianchi, P. Marovino, A.M. Paoletti, G. Padeletti, G. Pennesi, G. Rossi, Thin Solid Films 382 (2001) 74.
[125] J.P. Collman, C.E. Barnes, P.N. Swepston, J.A. Ibers, J. Am. Chem. Soc. 106 (1984) 3500.
[126] M. Hanack, Mol. Cryst. Liq. Cryst. 105 (1984) 133.
[127] M. Hanack, J. Osio Barcina, J. Pohmer, E. Witke, Mater. Res. Soc. Symp. Proc. 328 (1994) 233.
[128] M. Hanack, Mater. Sci. Forum 191 (1995) 13.
[129] M. Hanack, Mol. Cryst. Liq. Cryst. 160 (1988) 133.
[130] F. Mendizabal, J. Mol. Struc. Theochem 579 (2002) 169.
[131] M. Hanack, M. Lang, Adv. Mater. 6 (1994) 819.
[132] E. Orti, M.C. Piqueras, R. Crespo, J.L. Bredas, Chem. Mater. 2 (1990) 110.
[133] A. Rager, B. Gompf, L. Duerselen, H. Mockert, D. Schmeisser, W. Goepel, J. Mol. Electron. 5 (1989) 227.
[134] W. Goepel, Synth. Met. 41 (1991) 1087.
[135] A. Capobianchi, M. Tucci, Thin Solid Films 451–452 (2004) 33.
[136] A. Pauly, J.P. Germain, J.P. Blanc, Electron Technol. 33 (2000) 179.
[137] G. Guillaud, J. Simon, J.P. Germain, Coord. Chem. Rev. 178–180 (1998) 1433.
[138] A. Generosi, V.R. Albertini, G. Rossi, G. Pennesi, R. Caminiti, J. Phys. Chem. B 107 (2003) 575.
[139] V. Rossi Albertini, A. Generosi, B. Paci, P. Perfetti, G. Rossi, A. Capobianchi, A.M. Paoletti, R. Caminiti, Appl. Phys. Lett. 82 (2003) 3868.
[140] A. Capobianchi, A.M. Paoletti, G. Pennesi, G. Rossi, Sensors and Microsystems, in: Proceedings of the Italian Conference, 1st, Rome, Feb. 19–20, 1996, p. 50.
[141] A. Generosi, B. Paci, V. Rossi Albertini, P. Perfetti, G. Pennesi, A. M. Paoletti, G. Rossi, A. Capobianchi, R. Caminiti, Appl. Phys. Lett. 86 (2005) 114106/1.
[142] A. Generosi, B. Paci, V. Rossi Albertini, P. Perfetti, A. M. Paoletti, G. Pennesi, G. Rossi, R. Caminiti, J. Appl. Phys. 99 (2006) 044901/1.
[143] A. Generosi, B. Paci, V. R. Albertini, P. Perfetti, A. M. Paoletti, G. Pennesi, G. Rossi, R. Caminiti, Appl. Phys. Lett. 88 (2006) 104106/1.
[144] V.V. Arslanov, Y.G. Gorbunova, S.L. Selektor, L.S. Sheinina, O.G. Tselykh, Y.Y. Enakieva, A.Y. Tsivadze, Russ. Chem. Bull. 53 (2004) 2532.
[145] X. Li, W. Xu, X. Wang, H. Jia, B. Zhao, B. Li, Y. Ozaki, Thin Solid Films 457 (2004) 372.
[146] X.-l. Li, W.-q. Xu, H.-y. Jia, X. Wang, B. Zhao, B.-f. Li, Y. Ozaki, Chem. Res. Chin. U. 20 (2004) 345.
[147] M. Ebadi, Can. J. Chem 81 (2003) 161.
[148] R.A. Sheldon, J. Mol. Catal. A: Chem. 107 (1996) 75.
[149] N. d'Alessandro, L. Liberatore, L. Tonucci, A. Morvillo, M. Bressan, New J. Chem. 25 (2001) 1319.
[150] N. d'Alessandro, L. Liberatore, L. Tonucci, A. Morvillo, M. Bressan, J. Mol. Catal. A: Chem. 175 (2001) 83.
[151] N. d'Alessandro, L. Tonucci, M. Bressan, L.K. Dragani, A. Morvillo, Eur. J. Inorg. Chem. (2003) 1807.
[152] N. d'Alessandro, L. Tonucci, M. Bonetti, M. Di Deo, M. Bressan, A. Morvillo, New J. Chem. 27 (2003) 989.
[153] M. Ebadi, Electrochim. Acta 48 (2003) 4233.
[154] M. Sekota, T. Nyokong, Electroanalysis 9 (1997) 1257.
[155] J.A.R. Van Veen, C. Visser, Electrochim. Acta 24 (1979) 921.
[156] J.A.R. Van Veen, J.F. Van Baar, K.J. Kroese, J. Chem. Soc., Faraday Trans. 1 77 (1981) 2827.
[157] M. Shibata, N. Furuya, J. Electroanal. Chem. 507 (2001) 177.
[158] M. Ebadi, A.B.P. Lever, J. Porphyrins Phthalocyanine 7 (2003) 529.
[159] M. Shibata, N. Furuya, Electrochim. Acta 48 (2003) 3953.
[160] L.J. Boucher, E.J. Dadey, D.R. Spears, Proc. Int. Conf. Coal Sci. (1983) 763.
[161] H.-H. Liu, Y. Wang, Y.-J. Shu, X.-G. Zhou, J. Wu, S.-Y. Yan, J. Mol. Catal. A: Chem. 246 (2006) 49.
[162] A.P. Castano, T.N. Demidova, M.R. Hamblin, Photodiag. Photodyn. Ther. 1 (2004) 279.
[163] M.J. Clarke, Coord. Chem. Rev. 232 (2002) 69.
[164] P. Charlesworth, T.G. Truscott, R.C. Brooks, B.C. Wilson, J. Photochem. Photobiol. B 26 (1994) 277.
[165] Michael Graetzel Festschrift, a tribute for his 60th Birthday, Dye Sensitized Solar Cells, Coord. Chem. Rev. 248 (2004) issues 13 and 14.
[166] M.K. Nazeeruddin, R. Humphry-Baker, M. Grätzel, B.A. Murrer, Chem. Commun. (1998) 719.
[167] G. Liu, A. Klein, A. Thissen, W. Jaegermann, Surf. Sci. 539 (2003) 37.